

# Photoprocesses of Copper Complexes That Bind to DNA

David R. McMillin\* and Kristina M. McNett

Department of Chemistry, Purdue University, West Lafayette, Indiana 47907-1393

Received October 13, 1997 (Revised Manuscript Received February 16, 1998)

## Contents

I. Context of the DNA Studies	1201
A. Relevance of Photochemistry	1201
B. Elements of DNA Structure	1202
C. Ligand Binding Interactions	1202
D. Copper Phenanthrolines as Artificial Nucleases	1203
II. Photochemistry of $\text{Cu}(\text{NN})_2^+$ Systems	1204
A. Nature of the $\text{Cu}(\text{NN})_2^+$ Chromophore	1204
B. Flattening Distortions	1204
C. Environmental Effects	1205
III. Photophysics of $\text{Cu}(\text{NN})_2^+$ Systems Interacting with DNA	1206
A. Experimental Design	1206
B. $\text{Cu}(\text{dmp})_2^+$	1206
C. $\text{Cu}(\text{bcp})_2^+$	1206
D. $\text{Cu}(\text{dmpp})_2^+$	1207
E. Summary of Copper Phenanthrolines	1207
IV. Copper Porphyrins	1208
A. Structures	1208
B. Relevance to DNA	1208
C. Early Photochemistry	1208
D. New Aspects of the Photochemistry	1209
E. Exciplex Formation	1211
V. Copper Porphyrins and DNA	1212
A. Binding Interactions	1212
B. Specificity	1213
C. Structure of the Adducts	1213
D. Luminescence Studies	1214
E. Hairpin Hosts	1215
F. Transient Raman Studies	1216
G. Summary	1217
VI. Acknowledgments	1217
VII. References	1218



David R. McMillin received his B.A. in Chemistry from Knox College in 1969. He went on to obtain a Ph.D. in Inorganic Chemistry in 1973 from the University of Illinois where he studied in the area of coordination chemistry under the direction of the late Russell S. Drago. From there he moved to the California Institute of Technology to do postdoctoral work with Harry B. Gray in the field of bioinorganic chemistry. In 1975, Dr. McMillin joined the faculty at Purdue University. There he has worked mainly on problems in the areas of copper-containing proteins and inorganic photochemistry. He discovered a novel type of exciplex formation which is becoming increasingly evident in the chemistry of the photoexcited states of late transition metal ions. Pioneering work by David S. Sigman with copper phenanthrolines that act as artificial nucleases stimulated Dr. McMillin's current efforts in using luminescence techniques to investigate DNA-binding interactions.



Kristina M. McNett was born in Sylvania, OH. As an undergraduate, her research centered around electron microscopy under the direction of Dr. M. Kordesich in the Physics Department at Ohio University. She also spent a summer at the University of Toledo on an NSF–REU project on solar cells. After graduating in 1994 with a B.S. in physics and a B.S. in chemistry from the Honors Tutorial Program at Ohio University, she joined Dr. D. McMillin's laboratory at Purdue University. Her Ph.D. research revolves around copper(II) porphyrins.

way of detecting DNA in electrophoresis gels,<sup>1</sup> and redox-active excited states are useful as nonspecific

## I. Context of the DNA Studies

### A. Relevance of Photochemistry

This review focuses on recent studies of the photophysical properties of two classes of copper complexes that are of interest because of their DNA-binding interactions. The work represents a subset of a larger effort concerned with utilizing photochemical methodology to explore the chemistry of DNA. A brief listing of some applications will illustrate the breadth of the field. For example, the fluorescent indicator ethidium bromide provides a convenient

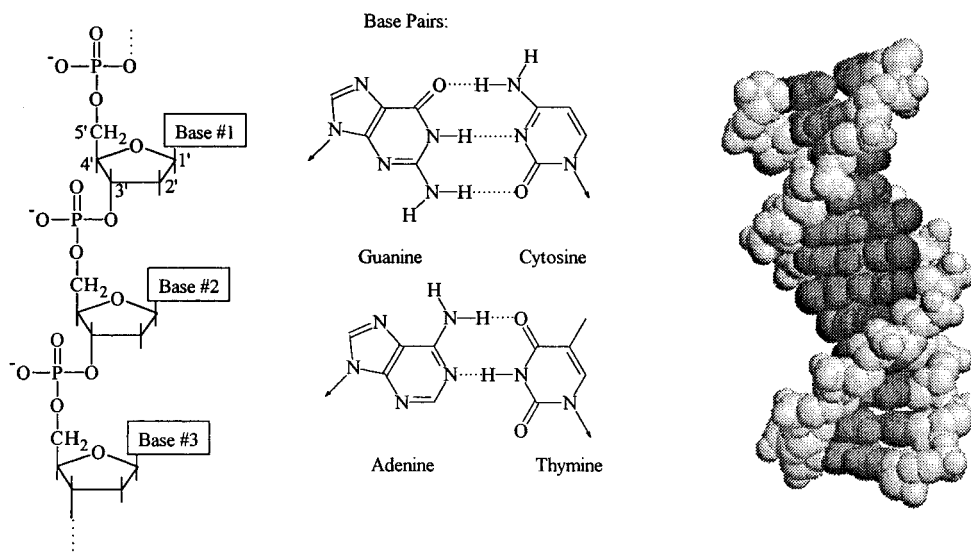


**Figure 1.** Representations of an oligonucleotide chain (left), A=T and G=C base pairs (middle), and B-form DNA with its major and minor grooves (right). The lightly shaded atoms correspond to the sugar-phosphate backbone.

nucleases for mapping the "footprints" of DNA- or RNA-binding proteins.<sup>2,3</sup> In medicine photodynamic therapy is a promising method,<sup>4</sup> and one strategy for combating diseased cells is to photosensitize reactions involving DNA. Photoactive metal complexes can also act as spectroscopic reporter probes for relaying information about DNA conformation.<sup>5</sup> Many of the applications mentioned above depend on a binding interaction between the DNA and a chromophore; hence developments in these areas could lead to advances in drug design. In the particular case of copper complexes, the luminescence (fluorescence and phosphorescence) properties are often quite sensitive to the local environment, and they can provide unique information about binding interactions.

## B. Elements of DNA Structure

For the present purposes it is useful to view DNA as a double-helical assembly of two polynucleotides held together by hydrogen bonding and hydrophobic forces. Each polynucleotide includes a backbone of 2'-deoxyribose and phosphate moieties condensed together to form an alternating polymer (Figure 1). The phosphodiester links involve the 5' and 3' oxygens of the sugar, and as a result, the polymer normally has terminal 5'- and 3'-phosphate ends. In addition, each sugar residue in the chain has a purine or a pyrimidine base covalently linked to its C1' carbon. Under normal circumstances in aqueous solution the bases tend to stack one upon the other along the chain, and in standard B-form DNA two complementary chains come together to form a duplex. The inside of the duplex contains a column of complementary base pairs (Figure 1). In the extended chain, the phosphate-phosphate distance is about 6 Å, but the thickness of a typical base is only about 3.3 Å. Thus, there has to be a horizontal displacement of the phosphate groups in order for stacking to occur.<sup>6</sup> As a consequence, each sugar-phosphate backbone winds around the column of base pairs in a helical fashion. The twist angle between the long axes of adjacent base pairs is around 32°,

and a stack of about 11 base pairs makes a complete turn of double helix. In a crude fashion one can view B-form DNA as a twisted ladder with the base pairs as the rungs and the sugar-phosphate chains as the sides. The C1'-N bonds that link the bases to the deoxyribose units occur at an angle with respect to the long axis of the base pair; hence the C1'-C1' vector that connects the two sugars lies off the axis toward one of the edges of the base pair. Consequently, the spacing between the sugar-phosphate chains is not uniform up and down the helix, and there are two different types of "grooves" that wind along the surface of the DNA duplex. The minor groove has a depth of about 7.5 Å and a width of 5.7 Å, while the major groove has a nominal depth of 8.5 Å and a width of 11.7 Å. The deoxyribose groups form the walls of the grooves and the opposite edges of the base pairs form the floors. Although the phosphate groups attract an atmosphere of cations that partially neutralizes the charge, there is a residual electric field that is relatively strong within the minor groove.

There are two other important, but less common forms of double-helical DNA. So-called A-form DNA entails a different sugar conformation and represents a coiled form of a double helix. In this structure the major groove is narrower and deeper, and the bases are no longer perpendicular to the helix axis. Double-helical RNA commonly adopts this conformation. The third structure, Z-form DNA, is left-handed. At high ionic strengths sequences that involve alternating runs of cytosine and guanine bases tend to adopt this structure.

## C. Ligand Binding Interactions

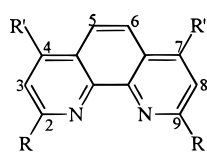
Adducts formed from metal complexes and DNA range from covalently to noncovalently bound and for the latter the degree of internalization can vary markedly. The simplest type of noncovalent adduct is essentially an outer-sphere assembly involving a cationic complex and the negatively charged DNA molecule. The aquated ions of sodium and magne-

sium associate with DNA in this fashion, and molecules such as  $\text{Ru}(\text{bpy})_3^{2+}$  may as well.<sup>7</sup> (bpy = 2,2'-bipyridine) As with any other charged surface, one can describe the ionic atmosphere of DNA in terms of two layers. The inner layer is the more tightly bound and compact; it consists of a sheath of water molecules and counterions that neutralize something like 50–75% of the charge density due to the phosphate groups. The outer layer bridges the transition to the bulk phase and consists of a more diffuse array of counterions as well as anions in a secondary solvation shell. Some types of ions bind more specifically in groove regions. For example, a recent NMR study suggests that  $\text{Pt}(\text{en})_2^{2+}$  binds near a 5'AT3' step in the minor groove of a DNA duplex formed from a self-complementary oligonucleotide that contains 12 residues (a 12-mer).<sup>8</sup> (en = ethylenediamine) On the other hand,  $\text{Co}(\text{en})_3^{3+}$  appears to bind near a 5'GG3' step in the major groove of another duplex.<sup>9</sup> Aside from the shape of the cation, factors that influence the binding include the local electric field of the DNA, van der Waals forces, potential hydrogen-bonding interactions with atoms on the DNA molecule, and hydrophobic effects. The latter derive in large part from the increase in entropy that occurs when adduct formation results in the release of water molecules from within the groove of DNA and/or from the surface of the probe ion. A more intimate type of noncovalent binding, known as intercalation, occurs when the double helix unwinds enough to open a slot between adjacent base pairs and permits the insertion of a fused-ring aromatic system.<sup>10</sup> The basic forces involved are the same for groove binding and intercalation; it is only a question of what combination produces the energy minimum in the overall configuration space. The structure of  $\text{Pt}(\text{trpy})(\text{HET})^+$  in combination with the  $[\text{d}(\text{CpG})]_2^{2-}$  miniduplex is an example of an intercalated complex.<sup>11</sup> (trpy = 2,2':6',2''-terpyridine and HET = 2-hydroxyethanethiolate) More recently, Williams and co-workers have solved the crystal structure of a cationic copper porphyrin intercalated into a duplex formed by the palindromic oligonucleotide d(CGATCG).<sup>12</sup> A detailed discussion of this adduct will appear below. Other platinum complexes bind covalently. Recently, Takahara et al. have described the crystal structure of the duplex  $\text{d}(\text{CTCTGGTCTCC})\cdot\text{d}(\text{GGAGACCAGAG})$  with  $\text{Pt}(\text{NH}_3)_2^{2+}$  coordinated to the N7 nitrogens of the G<sub>5</sub> and G<sub>6</sub> residues.<sup>13</sup> Huang et al. have described the solution structure of a different adduct of  $\text{Pt}(\text{NH}_3)_2^{2+}$  with a small duplex.<sup>14</sup> In this case, the platinum moiety forms an interstrand cross-link between two guanines. Finally, it is prudent to recognize the fact that DNA is a multifaceted host that can stimulate aggregation of the guest ion.<sup>15,16</sup> Condensation equilibria vary with the nature of the guest ion and the conditions, e.g., such things as the ionic strength and the ratio of drug to nucleotide in solution.

#### D. Copper Phenanthrolines as Artificial Nucleases

Sigman and co-workers discovered the first efficient artificial nuclease that acts via an essential, nonco-

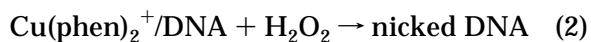
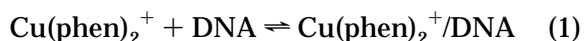
Chart 1



	R	R'
phen	H	H
dmp	Me	H
bap	H	Ph
bcp	Me	Ph

valently bound intermediate, and they showed that  $\text{Cu}(\text{phen})_2^+$  was the precursor.<sup>17–19</sup> (phen = 1,10-phenanthroline; see Chart 1). This was a serendipitous finding because they were originally investigating the zinc requirement of a DNA polymerase. Under normal laboratory conditions, the presence of a copper ion, phen, and a reducing agent such as a thiol are necessary for the nuclease activity. Hydrogen peroxide generated in situ is an obligatory intermediate because the presence of catalase abolishes the activity. Scheme 1 is a simplified representation of some of the key steps in the overall reaction:

Scheme 1



where the slash denotes a noncovalent binding interaction between the copper complex and the DNA molecule. Analysis of the cleavage products reveals that the cleavage results from sugar oxidation. Although Fenton-type chemistry seems plausible, several lines of evidence indicate that the free hydroxyl radical is not the oxidant.<sup>17,18</sup> When the hydroxyl radical is the oxidant, hydrogen atom abstraction occurs equally efficiently at the C1' and C4' carbons of the ribose group; however, the copper system shows a strong preference for attack at the C1' carbon.<sup>20</sup> The charge of the copper complex matters because there is no activity if the phen ligand has a carboxylate group tethered to the C5 carbon.<sup>21</sup> In addition, the sequence-specific nature of the cutting provides strong evidence that a binding event is central to the scission mechanism. The oxidizing intermediate probably involves some type of  $\text{Cu}(\text{OH})^{2+}$  moiety. Loss of a phenanthroline ligand may occur prior to the reaction with hydrogen peroxide,<sup>18</sup> consistent with the notion that hydrogen peroxide generally reacts by an inner-sphere mechanism. The oxidizing intermediate probably has a short lifetime and may not achieve an equilibrium distribution along the DNA polymer. If so, the binding equilibria involving  $\text{Cu}(\text{phen})_2^+$  may account for the cutting pattern.

There is no definitive information available about the structure of the  $\text{Cu}(\text{phen})_2^+/\text{DNA}$  associate, but various observations provide clues. In view of the cutting data, the copper complex may lodge in the minor groove where the C1' and C4' hydrogens lie. Substituent effects are consistent with the idea that one of the phen ligands enters the groove in a side-on fashion. Thus, Sigman and co-workers have found that substitution on the backside of the phen ligand, i.e., at the C5 position, has a minor influence on the

cutting activity but that the introduction of methyl substituents in the C3 and C8 positions sharply reduces the activity.<sup>18</sup> On the other hand, Veal and Rill have concluded that some type of partial intercalation occurs.<sup>22</sup> In particular, they have found that the addition of  $\text{Cu}(\text{phen})_2^+$  enhances the specific viscosity due to the DNA in solution, presumably because of the elongation of the rodlike molecules in solution. In the minor groove this is most feasible if the back edge of one of the phenanthroline ligands wedges between two adjacent base pairs. They have also reported that the interaction with the DNA enhances the charge-transfer absorption intensity that occurs in the vicinity of 525 nm. As will become apparent below, this is consistent with a flattening distortion and possibly particle formation. In the case of the more hydrophobic complex  $\text{Cu}(\text{bap})_2^+$ , Sigman and co-workers have also concluded that intercalative binding may occur because DNA scission occurs at a significantly reduced rate and with less sequence specificity by comparison with  $\text{Cu}(\text{phen})_2^+$ .<sup>23</sup> (bap = 2,9-diphenyl-1,10-phenanthroline; see Chart 1.)

The introduction of the dmp ligand, where dmp denotes 2,9-dimethyl-1,10-phenanthroline, is useful in experimental work because it abolishes the cutting reaction. One reason is that methyl substituents in the 2 and 9 positions dramatically stabilize the copper(I) oxidation state and reduce the reactivity with oxidizing agents.<sup>24</sup> For steric reasons these groups could also modify the binding constant and the adduct geometry.<sup>18</sup> The binding interactions of the methyl-substituted systems are of interest because they show photoluminescence under certain conditions. After a brief synopsis of the photochemistry and photophysics of these copper systems, a review of the results obtained with DNA-containing solutions follows.

## II. Photochemistry of $\text{Cu}(\text{NN})_2^+$ Systems

### A. Nature of the $\text{Cu}(\text{NN})_2^+$ Chromophore

The understanding of the electronic properties of  $\text{Cu}(\text{NN})_2^+$  systems, where NN is a chelating heteroaromatic ligand like 1,10-phenanthroline, has progressed markedly in recent years. In solution the symmetry is approximately  $D_{2d}$ , and the electronic configuration of the metal center is  $d^{10}$ . As a result the lowest energy excited state is a  $d-\pi^*$  charge-transfer (CT) state. Comparisons with the well-known  $\text{Ru}(\text{bpy})_3^{2+}$  system reveal some of the unique aspects of the copper(I) complexes. With either copper or ruthenium, the excitation occurs from what in cubic symmetry would be a triply degenerate set of orbitals rich in d-orbital character. In reality the symmetry is lower (Figure 2), and with each system the intense visible absorption band arises from excitation out of a doubly degenerate e level.<sup>25,26</sup> In the  $D_3$  symmetry of  $\text{Ru}(\text{bpy})_3^{2+}$ , a  $\pi$ -back-bonding interaction with empty  $\pi^*$  orbitals of the ligand stabilizes the e sublevel relative to the  $a_1$  sublevel.<sup>25</sup> In the  $D_{2d}$  copper(I) systems, the  $t_2$  orbitals split into e and  $b_2$  species.<sup>27-29</sup> Although a stabilizing  $\pi$ -back-bonding interaction with ligand orbitals of e sym-

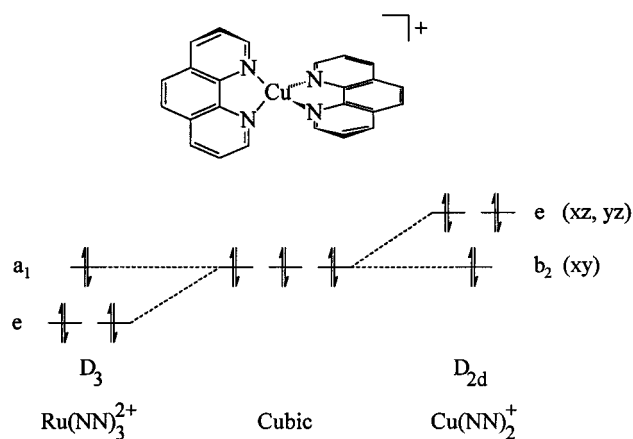


**Figure 2.** Relative energies of the three highest occupied d orbitals of a low-spin  $d^6$  complex in  $D_3$  symmetry or a  $d^{10}$  complex in  $D_{2d}$  symmetry. The idealized  $\text{Cu}(\text{phen})_2^+$  system has  $D_{2d}$  symmetry with the  $z$  axis bisecting each ligand.

metry occurs in this system as well, a  $\sigma$ -antibonding interaction has an overriding influence.<sup>28</sup> Due to the small bite of the ligand (the N–Cu–N angle is  $82 \pm 1^\circ$  at each phenanthroline<sup>30</sup>), the  $xz$  and  $yz$  orbitals of the copper experience significant overlap with the lone-pair orbitals of the chelate nitrogens. This drives the doubly degenerate e level to higher energy, in the same way that a distortion known as a tetrahedral elongation does. In reality, the thermally equilibrated excited states of each system adopt lower symmetry, at least in solution. One reason is that the excited-state develops a dipole moment (i.e.,  $\text{Cu}^{2+}-(\text{NN})^-$  character) and one of the ligands becomes unique as the excited electron localizes in its  $\pi^*$  orbital.<sup>31</sup> Since the ground state does not have a dipole moment, polar solvents differentially stabilize the CT state and induce a red shift in the emission that varies with the dielectric constant of the solvent.<sup>32</sup>

### B. Flattening Distortions

Due to the fact that the “hole” created during the CT excitation occurs in a metal–ligand,  $\sigma$ -antibonding orbital, another more significant distortion occurs in the vibrationally relaxed excited state. In particular, the development of copper(II) character in the excited-state encourages a flattening distortion.<sup>28,32-34</sup> As illustrated in Figure 3, the consequences of the distortion include a decrease in the energy available in the excited state and a reduction of the excited-state lifetime. Steric forces limit the extent of the distortion, especially when there are bulky substituents in the 2,9 positions of the phenanthroline ligand. Thus, in methylene chloride the lifetime and the emission energy increase as the size of the substituent in the 2,9 positions increases (Table 1).<sup>32</sup> The distortion is evidently so great in the case of  $\text{Cu}(\text{phen})_2^+$  that to date there are no reports of luminescence, even from a rigid, low-temperature glass.<sup>33,34</sup>

The restoring force that resists the flattening is very modest, and even in the ground-state significant distortions can occur in the solid state as a result of packing forces.<sup>35,36</sup> The  $[\text{Cu}(\text{dnpp})_2]\text{PF}_6$  system is a particularly interesting case because it reveals the

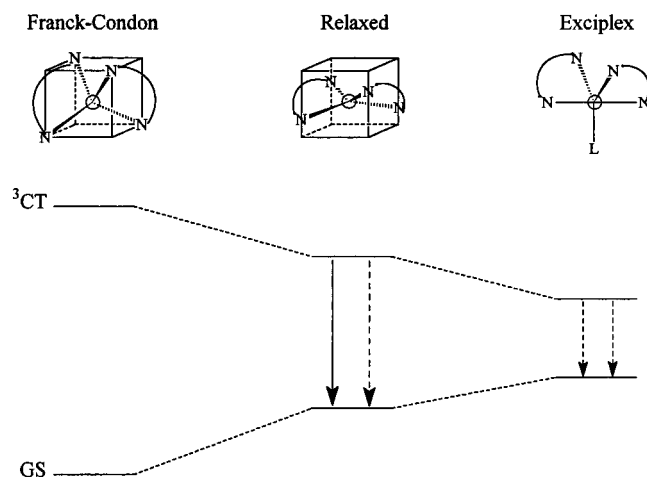


**Figure 3.** The influences that a  $D_2$ -flattening distortion and formation of a five-coordinate adduct have on the relative energies of the ground state and the lowest energy CT state of a copper phenanthroline. The solid arrow denotes a radiative decay pathway, and the dashed arrows denote nonradiative processes. Because of the time scales involved, flattening probably occurs prior to attack by a Lewis base.

**Table 1. Emission Data from  $\text{Cu}(2,9\text{-R}_2\text{-phen})_2^+$  Systems in Deoxygenated Solutions<sup>a</sup>**

R group	$10^4 \times \phi^b$	$\lambda_{\text{max}}^{\text{em}}, \text{nm}^c$	$\tau, \text{ns}$		
			$\text{CH}_2\text{Cl}_2$	THF	$\text{CH}_3\text{CN}$
$-\text{CH}(\text{CH}_3)(\text{C}_2\text{H}_5)$	45	650	400	200	130
$-\text{CH}_2\text{C}(\text{CH}_3)_3$	16	665	260	140	100
$-(\text{CH}_2)_7\text{CH}_3$	10	673	155	55	50
$-(\text{CH}_2)_3\text{CH}_3$	9	670	150	50	35
$-\text{CH}_3$	4	690	90	—	$2^d$
$-\text{H}$	—	—	—	—	—

<sup>a</sup> Except as noted data from Eggleston, M. K.; McMillin, D. R.; Koeng, K. S.; Pallenberg, A. J. *Inorg. Chem.* 1997, 36, 172–176. <sup>b</sup> Emission yield in  $\text{CH}_2\text{Cl}_2$ . <sup>c</sup> Uncorrected emission maximum in  $\text{CH}_2\text{Cl}_2$ . <sup>d</sup> Palmer, C. E. A.; McMillin, D. R.; Kirmaier, C.; Holten, D. *Inorg. Chem.* 1987, 26, 3167–3170.

extent of the distortion that can occur in the excited state. (dnpp = 2,9-dineopentyl-1,10-phenanthroline.) The X-ray structure reveals that the dihedral angle between the least-squares planes of the dnpp ligands is only  $63.4(1)^\circ$ . Such flattening is feasible only because of the packing forces that control the conformations of the neopentyl substituents. What makes this system especially interesting is the fact that the emissions from the solid and solutions maximize at almost the same wavelength. This is quite unusual because the solution emission usually appears at a significantly longer wavelength.<sup>36</sup> In view of the limited opportunity for structural relaxation in the solid state, this means that the structure in the crystal very probably mimics the one that the vibrationally relaxed CT excited-state adopts in solution. Finding this benchmark structure in the solid was a fortuitous result because absorbance data reveal that the ground-state dnpp complex adopts a normal  $D_{2d}$ -like geometry in solution.<sup>36</sup>

### C. Environmental Effects

In addition to the substituents, the local environment has a profound influence on the lifetime of the

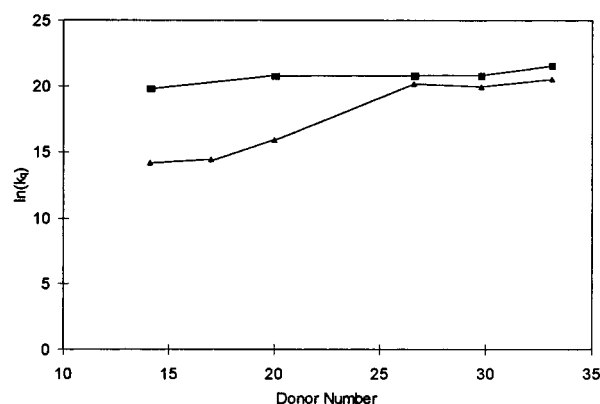


**Figure 4.** Correlation between the quenching rate constants and base strength as measured by the Gutmann donor numbers. The triangles represent data for the  $\text{Cu}(\text{dmp})_2^+$  system,<sup>41</sup> and the squares relate to the  $\text{Cu}(\text{TPP})$  system, vide infra.

excited state of a  $\text{Cu}(\text{NN})_2^+$  system. Donor media generally quench the lifetime, as one can see with  $\text{Cu}(\text{dbp})_2^+$ . The data in Table 1 show that the CT excited state lifetime drops from 150 ns in the weakly donating solvent methylene chloride to 35 ns in acetonitrile, a modestly basic solvent. In the case of the dmp complex, the same change in solvent induces a drop in the lifetime of well over an order of magnitude.<sup>37</sup> There is overwhelming evidence that the quenching reaction involves associative attack by the solvent. The reaction is favorable because the CT excitation entails a formal increase in the oxidation state of the copper center, and copper(II) compounds are frequently five-coordinate. For example, a related bis-bipyridine complex of copper(II) crystallizes as a five-coordinate complex even in the presence of a weakly coordinating anion like perchlorate.<sup>38</sup> In addition, EXAFS studies show that  $\text{Cu}(\text{dmp})_2^+$  picks up an extra ligand upon oxidation.<sup>39</sup> Coordination of a fifth ligand stabilizes the CT excited state and destabilizes the ground state, which inevitably promotes quenching (Figure 3).<sup>40–42</sup> This is a type of exciplex quenching, where the term exciplex is short for excited-state complex. Quenching constants measured in methylene chloride are consistent with the proposed mechanism and increase with the donor strength of the quencher, as measured by the Gutmann donor number (Figure 4).<sup>41</sup> An analysis of steric effects also supports the exciplex mechanism.<sup>32,43</sup> Thus, introduction of steric bulk on either the copper center or the Lewis base inhibits the quenching process. Furthermore, the activation enthalpy for quenching photoexcited  $\text{Cu}(\text{dmp})_2^+$  tends to be negative for weak donors.<sup>41</sup> This is consistent with the existence of a reversible, bond-making process prior to the deactivation step. The same mechanism accounts for the fact that the excited-state lifetime of the dmp complex varies with the nucleophilicity of the counterion in a low dielectric solvent like methylene chloride.<sup>44</sup> Finally, theoretical calculations reveal that the addition of a fifth ligand is a favorable process.<sup>28</sup> By analogy with authentic copper(II) analogues, the adduct probably involves a trigonal-bipyramidal coordination geometry with the entering base in one of the equatorial positions.<sup>40</sup>

Aside from the basicity, the rigidity of the local environment plays an important role. Consider the  $\text{Cu}(\text{NN})_2^+$  complex with (*N*-*o*-toluidino)methyl groups in the 2,9 positions of the phenanthrolines. The CT emission is prominent and exhibits a lifetime of 3.8  $\mu\text{s}$  in a rigid (alcohol) glass at 90 K, but there is virtually no detectable emission in fluid solution, even in a solvent like methylene chloride.<sup>33</sup> Almost certainly the quenching occurs as a result of a structural reorganization in fluid solution that leads to formation of an intramolecular exciplex via the coordination of a toluidine nitrogen. In a rigid medium the same process does not occur, and the size of the substituents inhibits the usual flattening distortion. This accounts for the relatively long lifetime of the CT state in the glass. In the case of  $\text{Cu}(\text{dmp})_2^+$  there is only a hint of emission from an alcohol solution at room temperature, but the complex emits nicely in a glass ( $\tau = 570$  ns at 90 K).<sup>33,45</sup> Here the rigidity of the low-temperature glass prevents associative attack by the solvent and, hence, exciplex quenching. In principle, adduct formation with a macromolecule like DNA can also influence exciplex formation by altering the conformational flexibility and/or the steric requirement for ligand addition. This notion led to the use of luminescence techniques to investigate DNA-binding interactions.

### III. Photophysics of $\text{Cu}(\text{NN})_2^+$ Systems Interacting with DNA

#### A. Experimental Design

The luminescence experiments involving copper phenanthrolines and DNA depend on a number of considerations including solubility and oxygen sensitivity. In view of the work of Sigman and co-workers,<sup>17,18</sup> the  $\text{Cu}(\text{phen})_2^+$  system would be the most interesting, but the complex is nonemissive in solution as noted earlier. The dmp analogue is, however, a close facsimile and is quite stable as  $\text{Cu}(\text{dmp})_2^+$  in the presence of air. Recent studies justify binding studies of the dmp complex in their own right, because the complex acts as a transcription inhibitor, apparently by binding to single-stranded regions of DNA exposed as a result of interaction with RNA polymerase.<sup>17,46</sup> The bcp ligand defined in Chart 1 provides an air-stable analogue of  $\text{Cu}(\text{bap})_2^+$ . For solubility reasons, in aqueous media it is convenient to introduce the copper complexes as chloride salts. Even so, the complex with the aryl substituents is relatively insoluble except in mixed solvents containing, for example, 20–30% alcohol.<sup>47a</sup> Analogous problems also arise with the octahedral ruthenium(II) complexes involving comparable ligands.<sup>48</sup> A straightforward method of preparing solutions is to introduce the chromophore via an aliquot of a stock solution in alcohol. However, this can result in the production of a colloidal suspension that may appear to be homogeneous.<sup>47a</sup> The difficulties that can arise are evident from the fact that a solution of  $\text{Cu}(\text{bcp})_2^+$  prepared in this way exhibits a relatively intense CT photoluminescence when the mixture is 6 vol % MeOH, but not 33% MeOH.<sup>47a</sup> Both solvent systems are capable of quenching photoexcited copper phenan-

throlines, but the solution containing 6% MeOH is a colloidal suspension. Emission polarization studies expose the problem. Under normal conditions, in a solvent like methylene chloride, the polarization ratio of the emission is 0.004. However, in the 6% MeOH solution, the emission polarization ratio is 0.37 which implies that virtually no reorientation of the emitter occurs during the excited-state lifetime.<sup>47a</sup> The explanation is that the polarized emission comes from slowly rotating particulate matter. In the aggregate the lattice structure insulates the bulk chromophore from solvent attack. Under some conditions the introduction of polyelectrolytes such as poly(styrenesulfonate), or PSS, can induce a similar condensation process in what would otherwise be a homogeneous solution.<sup>47a</sup> For example, the addition of stoichiometric amounts of PSS to a 33% MeOH solution containing  $\text{Cu}(\text{bcp})_2^+$  induces a similar emission with a high polarization ratio. However, the addition of excess PSS disperses the copper complex once again, so that the emission signal practically vanishes. As discussed below, the addition of DNA can induce a similar effect. Note that introducing alcohol can induce a transition to A-form DNA; however, this requires much higher percentages of alcohol.<sup>47b</sup>

#### B. $\text{Cu}(\text{dmp})_2^+$

Some time ago, Tamilarasan and McMillin investigated the interaction between  $\text{Cu}(\text{dmp})_2^+$  and salmon testes (ST) DNA in 33% MeOH.<sup>16</sup> They found clear evidence of adduct formation in that the CT absorption showed hypochromism in the visible spectrum. In fact, the effect was larger than that associated with the CT absorption of  $\text{Cu}(\text{phen})_2^+$ . The bound complex was nevertheless solvent accessible because the solution yielded no significant CT emission intensity.<sup>47a</sup> In addition, uptake induced little, if any CD intensity in the CT absorption region.<sup>16</sup> For all intents and purposes, the binding appeared to be completely external with a minimal degree of electronic interaction. More intimate binding may occur at different alcohol levels, however, because Graham et al. found that the introduction of the dmp complex can enhance the viscosity specific to the DNA in the solution.<sup>49</sup> They attributed this to partial intercalation and elongation of the DNA molecules in solution.

#### C. $\text{Cu}(\text{bcp})_2^+$

The interaction with the bcp complex was of interest because it is an air-stable, potentially luminescent analogue of  $\text{Cu}(\text{bap})_2^+$ . In his studies, Sigman had reported that the bap system showed significantly reduced nuclease activity and less sequence specificity than the phen analogue.<sup>21</sup> He suggested that this was consistent with an alternative mode of binding, i.e., intercalation. Earlier, Barton and co-workers had reported that  $\text{Ru}(\text{bap})_3^{2+}$  was a much more avid binder than the parent phenanthroline complex and interpreted the results in terms of an intercalative binding model.<sup>50</sup>

Subsequent physical studies confirmed that the bcp complex interacted with DNA in a very different

fashion than the dmp analogue. One difference was that binding to DNA induced an even greater degree of hypochromism.<sup>16,47a</sup> With the bcp complex the binding interaction also produced a weak monosignate CD signal in the CT absorption region as well as a CT luminescence signal.<sup>16,47a,51</sup> Concentration-dependent studies established that at least two different types of adducts formed. At DNA-P/Cu < 8 (where DNA-P denotes the number of phosphate—or nucleic acid—residues in solution and Cu denotes the number of copper centers), the presence of the bcp complex induced a significant alteration of the CD spectrum in the UV region where the DNA absorbed.<sup>52</sup> However, at DNA-P/Cu > 30, the effect on the DNA signal was minor. There was also evidence of scattering artifacts in the emission spectrum at low DNA-P/Cu ratios.<sup>51</sup> At low ratios the presence of the DNA clearly induced some type of aggregation and/or microparticulate formation. Related effects occur with high loadings of aromatic dyes on polyanions and with hydrophobic intercalating agents such as proflavin.<sup>10,53</sup> On the other hand, introduction of excess DNA dispersed the chromophore because the scattering artifacts disappeared, and under these conditions it was reasonable to visualize the binding in molecular terms. The binding transition was also evident in the viscosity data.<sup>51</sup> At DNA-P/Cu ≥ 20, the interaction with Cu(bcp)<sub>2</sub><sup>+</sup> induced a 40–50% increase in the specific viscosity due to the DNA in solution.<sup>51</sup> However, at a DNA-P/Cu ratio of 10 or less the interaction with the bcp complex led to a reduction in the specific viscosity due to aggregation effects. Experiments with double-stranded RNA gave somewhat different results.<sup>54</sup> As with the DNA, the binding interaction with RNA induced hypochromism in the absorbance in the visible region and a weak signal in the CD spectrum. The bound form of the complex was also emissive. However, with RNA there was no increase in the specific viscosity at any nucleotide-to-copper ratio.

Partial intercalation of the complex with the incorporation of one of the bcp ligands between adjacent base pairs of the DNA may explain some of the observations. These include the viscosity enhancement and the inhibition of solvent-induced quenching. However, this mode of binding would almost certainly require one or more of the phenyl substituents to twist into the plane of the phenanthroline. Such a conformation is unstable, of course, because of hydrogen/hydrogen repulsive interactions. For example, in the solid state, the phenyl groups are well out of the plane, forming a dihedral angle of 63.2°.<sup>35</sup> This effect is probably responsible for the fact that the *N*-methyl-4,7-diphenyl-1,10-phenanthroline ion does not intercalate into DNA in contrast to related ions lacking phenyl substituents.<sup>55</sup> One way to minimize the steric problems would be to investigate a copper complex with only one phenyl substituent.

#### D. Cu(dmpp)<sub>2</sub><sup>+</sup>

In line with an observation by Barton and co-workers,<sup>56</sup> Meadows et al. investigated the interaction between Cu(dmpp)<sub>2</sub><sup>+</sup> and DNA in solution.<sup>57a</sup> (dmpp is 2,9-dimethyl-4-phenyl-1,10-phenanthroline.)

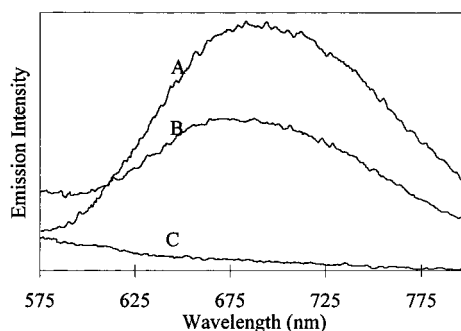


**Figure 5.** Uncorrected emission spectra measured in 20% MeOH at room temperature. The samples contained ST DNA with DNA-P/Cu = 50. The spectra are (A) Cu(bcp)<sub>2</sub><sup>+</sup>; (B) Cu(dmpp)<sub>2</sub><sup>+</sup>; and (C) Cu(dmp)<sub>2</sub><sup>+</sup>. (Reproduced with permission from ref 57b. Copyright 1994 Elsevier Science S.A.)

The idea is that partial intercalation might be more feasible if there were only one phenyl substituent on the backside of the phenanthroline. Figure 5 shows that there was an interaction and that the adduct exhibited CT emission. However, the signal was definitely weaker than the one obtained from the bcp complex.<sup>57b</sup> The adduct also exhibited a weak CD signal in the visible region. Viscometry data showed that the presence of the complex had no influence on the specific viscosity at low loadings and that the specific viscosity decreased at higher loadings (DNA-P/Cu ≤ 10).

#### E. Summary of Copper Phenanthrolines

The spectral properties of Cu(NN)<sub>2</sub><sup>+</sup> systems with phenyl substituents in the 4,7 positions are quite sensitive to the presence of DNA. Aggregation is a problem at low DNA-P/Cu ratios, but the presence of excess DNA disperses the copper complex. Under the latter conditions the CT absorption band exhibits a weak monosignate CD signal which suggests that the copper complex binds as a monomer. Adduct formation may entail partial intercalation, but this seems unlikely in view of the steric constraints. Moreover, there is no detectable increase in the specific viscosity when the dmpp complex binds to ST DNA or when the bcp complex binds to double-stranded RNA. At low loading levels, there is a viscosity increase when Cu(bcp)<sub>2</sub><sup>+</sup> binds to [poly(dA-dT)]<sub>2</sub>, but the increase is much greater than that induced by classical intercalators such as ethidium.<sup>51</sup> Nordén and co-workers have suggested that the observed results are compatible with partial intercalation;<sup>58</sup> however, it is still puzzling that the viscosity increase occurs in such a narrow range of systems. Some type of groove binding is an alternative possibility so long as this permits enhanced rigidity for the few systems such as [poly(dA-dT)]<sub>2</sub> that show an increase in the specific viscosity. The emission data also require that the degree of entanglement with the DNA be sufficient to inhibit solvent-induced expansion of the coordination number at copper. If the adduct is rigid enough, dissociation of the adduct may be necessary in order for exciplex quenching to occur. The latter scenario would also be consistent with the high emission polarization ratio observed for the bound complex.

Another model that can account for the physical data assumes that  $\text{Cu}(\text{bcp})_2^+$  is capable of bridging between two or more DNA molecules in solution.<sup>51</sup> One can view this type of adduct as a natural successor to the aggregates that occur at low DNA-P/Cu ratios. More effective intercalation will require molecules with a shape that is more compatible with insertion between base pairs. This was one motivation for subsequent studies involving a copper(II) porphyrin.

## IV. Copper Porphyrins

### A. Structures

A free-base porphyrin has two protonated nitrogens, but with deprotonation, the ligand normally acts as a dianionic, tetradentate macrocycle. To a first approximation, a porphyrin defines a plane of coordination, but ligand atoms readily move out of the plane as a result of doming, ruffling, or saddle distortions, to name a few.<sup>59</sup> Peripheral substitution is possible at the meso positions, as in  $\text{Cu}(\text{T4})$  in Charts 2 and 3, or at the  $\beta$  carbons of the four pyrrole moieties as in  $\text{Cu}(\text{OEP})$ . Due to contacts involving the ortho hydrogens of the substituents, the torsion

Chart 2

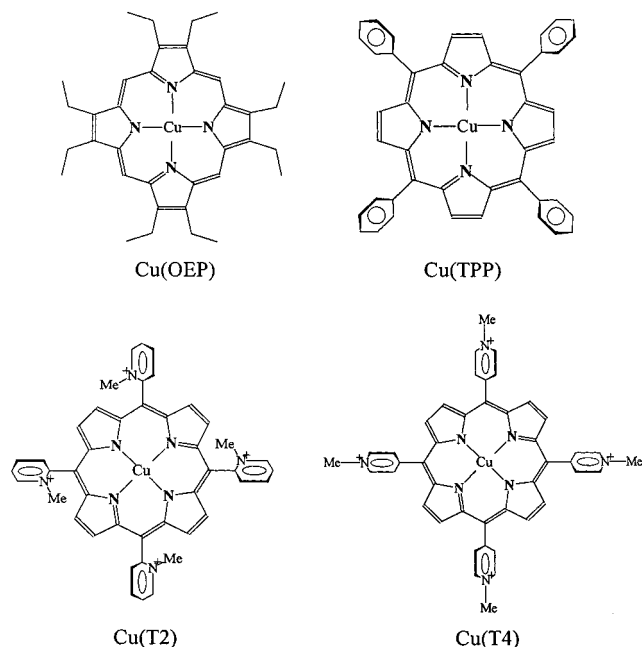


Chart 3

$\text{Cu}(\text{OEP})$	2,3,7,8,12,13,17,18-octaethylporphyrinatocopper(II)
$\text{Cu}(\text{TPP})$	5,10,15,20-tetraphenylporphyrinatocopper(II)
$\text{Cu}(\text{T2})$	5,10,15,20-tetra(N-methylpyridinium-2-yl)porphyrinatocopper(II)
$\text{Cu}(\text{T4})$	5,10,15,20-tetra(N-methylpyridinium-4-yl)porphyrinatocopper(II)
$\text{Cu}(\text{TCI2PP})$	5,10,15,20-tetra(2,6-dichlorophenyl)porphyrinatocopper(II)
$\text{Cu}(\text{TMP})$	5,10,15,20-tetra(2,4,6-trimethylphenyl)porphyrinatocopper(II)
$\text{Cu}(\text{TF5PP})$	5,10,15,20-tetra(pentafluorophenyl)porphyrinatocopper(II)
$\text{Cu}(\text{TCNPP})$	5,10,15,20-tetra(4-cyanophenyl)porphyrinatocopper(II)
$\text{Cu}(\text{TOMePP})$	5,10,15,20-tetra(4-methoxyphenyl)porphyrinatocopper(II)

angles of the pyridine moieties in the ligand  $\text{H}_2\text{T4}$  average about  $70^\circ$ .<sup>60</sup> The aryl substituents are fluxional,<sup>61</sup> but for steric reasons rotation can be very slow in derivatives such as  $\text{Cu}(\text{T2})$ .<sup>62</sup> The porphyrin core itself is quite hydrophobic, but substituents such as *N*-methylpyridinium impart a positive charge and enhance the solubility in water. Positively charged substituents obviously also enhance the DNA binding affinity. Almost without exception, copper(II) porphyrins are four-coordinate, i.e., they lack axial ligands.<sup>62</sup> On the other hand, zinc(II) derivatives tend to be five-coordinate,<sup>63</sup> and the Mn(III) and Fe(III) derivatives have one or more axial ligands as well.<sup>64</sup>

### B. Relevance to DNA

Part of the interest in metalloporphyrins stems from the potential for applications in the area of photodynamic therapy.<sup>5,65–67</sup> Since there is evidence that porphyrins spontaneously accumulate in malignant cells, another possible application involves using luminescence detection for diagnostic purposes.<sup>68</sup> Cationic porphyrins, such as  $\text{Cu}(\text{T4})$ , bind well to DNA, and this suggests that it may be possible to destroy a diseased cell by a photosensitization mechanism within the cell nucleus. Actually,  $\text{Cu}(\text{T4})$  itself is not a very effective photosensitizer due to its short excited-state lifetime.<sup>69</sup> The cytotoxicity actually derives from the production of singlet oxygen, and systems such as the free base  $\text{H}_2\text{T4}$  do this much better than  $\text{Cu}(\text{T4})$ .<sup>65,70</sup> However, the activity of an effective drug depends on a host of factors including the biodistribution, the mode of localization, the binding affinity in the vicinity of the target, the nature and specificity of the binding interaction, etc. A system like  $\text{Cu}(\text{T4})$  can be a very useful probe for the investigation of component steps within the overall scheme. In this regard, photophysical methods are useful tools for studying interactions involving  $\text{Cu}(\text{T4})$  as well as other metalloporphyrins. For example, Kelly and co-workers have investigated the DNA-binding interactions of  $\text{H}_2\text{T4}$  and  $\text{Zn}(\text{T4})$  by fluorescence techniques.<sup>71</sup> They have found that binding to  $[\text{poly}(\text{dA-dT})]_2$  sharpens the emission signal and enhances the intensity of the fluorescence of  $\text{H}_2\text{T4}$ . On the other hand, binding to  $[\text{poly}(\text{dG-dC})]_2$  decreases the emission intensity from the free base, but not  $\text{Zn}(\text{T4})$ ,<sup>71</sup> due to a difference in the mode of binding. Whereas the free base prefers to intercalate into GC sites, this is not possible for the zinc complex on account of the axial ligand. In the case of  $\text{Pd}(\text{T4})$ , Brun and Harriman have found that intercalation into DNA dramatically enhances the phosphorescence intensity from the complex.<sup>72</sup> Here internalization into the macromolecule protects the excited state from quenching by molecular oxygen. The free base  $\text{H}_2\text{T4}$  is capable of intercalating into DNA or binding externally, and action spectra show that energy transfer from DNA bases to the porphyrin is possible with either type of binding.<sup>73</sup>

### C. Early Photochemistry

Gouterman and co-workers have shown that a four-orbital model accounts for the visible spectra of



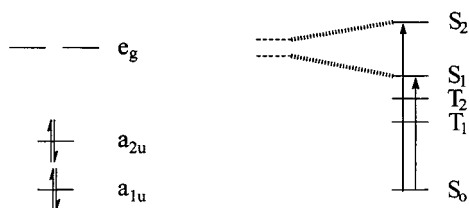


**Figure 6.** Energy levels in porphyrins. The levels on the left represent the two highest occupied molecular orbitals and the degenerate set of lowest unoccupied molecular orbitals in  $D_{4h}$  symmetry. The state diagram on the right depicts the relative energies of the ground state and lowest lying singlet and triplet  $\pi \leftarrow \pi^*$  excited states. The dashed lines represent the energies the two singlets would have in the absence of configuration interaction.

metalloporphyrins.<sup>74,75</sup> The orbitals involved are apparent in a simple Hückel model;<sup>76</sup> they correspond to the two highest occupied energy levels and the lowest unoccupied level which is doubly degenerate. In  $D_{4h}$  symmetry all four orbitals have  $\pi$  symmetry, and in the usual coordinate system the  $x$  and  $y$  axes extend along the metal–nitrogen bonds. Within this framework, the empty orbitals have  $e_g$  symmetry, and the two highest occupied orbitals span the  $a_{1u}$  and  $a_{2u}$  representations (Figure 6). The  $e_g \leftarrow a_{1u}$  and  $e_g \leftarrow a_{2u}$  excitations, each giving an  $E_u$  state, are both electric-dipole-allowed transitions with  $(x,y)$  polarizations. Contrary to what one might expect on the basis of the energy level scheme, these two lowest energy, spin-allowed transitions occur at very different energies and exhibit quite different intensities. The spread in the energies and the intensities is due to a configuration interaction between the two zero-order  $E_u$  states as a consequence of the electron–electron repulsion interaction (Figure 6).<sup>75</sup> The lower energy of the two spin-allowed transitions (the so-called Q band) occurs around 600 nm, and the other, much more intense transition, known as the Soret band, occurs around 400 nm. There are two associated triplet  $E_u$  states as well. In the case of a copper(II) porphyrin, which is paramagnetic, the triplet states exhibit a multiplet structure due to interactions with the unpaired electron in the metal  $d(x^2 - y^2)$  orbital.<sup>74</sup> The common designations of the multiplet states are the trip-doublet ( $^2T$ ) and trip-quartet ( $^4T$ ) states where the prefix “trip” denotes the intrinsic  $^3\pi \leftarrow \pi^*$  character of the excitation and the suffix designates the overall spin multiplicity. Often in solution studies the multiplet levels of the lowest energy excited state are in thermal equilibrium, and the whole population (the  $^{2,4}T$  system) decays with a single lifetime.<sup>77</sup>

The configuration interaction between the two  $^3E_u$  states is a much weaker effect; consequently, each has a dominant electronic configuration.<sup>75</sup> As a result, it is possible to label the corresponding multiplet systems as  $^{2,4}T(a_{2u})$  and  $^{2,4}T(a_{1u})$  according to the orbital origin of the excitation. Theory shows that the  $p\pi$  atomic orbitals of the pyrrole nitrogens play a significant role in the makeup of the  $a_{2u}$  molecular orbital as do the  $p\pi$  atomic orbitals of the meso carbon atoms (C5, C10, C15, and C20).<sup>74,75</sup> In contrast, the same set of  $p\pi$  atomic orbitals take no part in the  $a_{1u}$  molecular orbital. In Cu(TPP) the  $a_{2u}$  orbital is the highest occupied molecular orbital

**Table 2. Physical Data for Copper(II) Porphyrins**

complex	meso substituent	$E_0^a$ , V vs Cu(TPP) <sup>+0</sup>	$g_l^b$	$\tau$ , <sup>c</sup> ns
Cu(TCl2PP)	–2,6-Cl <sub>2</sub> -C <sub>6</sub> H <sub>3</sub>	0.03	2.190	300
Cu(TMP)	–2,4,6-Me <sub>3</sub> -C <sub>6</sub> H <sub>2</sub>	–0.02	2.185	220
Cu(TF5PP)	–C <sub>6</sub> F <sub>5</sub>	0.44	2.189	155
Cu(OEP)	–CH <sub>2</sub> CH <sub>3</sub> <sup>d</sup>	–0.24	2.190	110
Cu(TPP)	–H	0	2.189	40
Cu(TCNPP)	– <i>p</i> -CN-C <sub>6</sub> H <sub>4</sub>	0.11	2.180	25
Cu(TOMePP)	– <i>p</i> -(MeO)-C <sub>6</sub> H <sub>4</sub>	–0.17	2.183	15

<sup>a</sup> In methylene chloride containing 0.1 M TBAH. <sup>b</sup> From the powder spectrum in the free ligand host. <sup>c</sup> In deoxygenated methylene chloride at room temperature. <sup>d</sup> The eight ethyl substituents are on the  $\beta$  carbons of the pyrrole rings.

(HOMO), and the emission stems from the  $^{2,4}T(a_{2u})$  system.<sup>78</sup> On the other hand, in the case of Cu(TF5PP) the  $a_{2u}$  orbital falls below the  $a_{1u}$  because of the influence of the electron-withdrawing groups. (See Table 2 for the key to the porphyrin designations.) The same ordering occurs in the protoporphyrin Cu(OEP) due to the electron-donating ethyl substituents which drive up the energy of the  $a_{1u}$  level.<sup>79</sup> Because of the participation of the nitrogen  $p\pi$  orbitals in the  $a_{2u}$  orbital, the multiplet splitting is larger in systems such as Cu(TPP).<sup>74</sup> More specifically, the  $^2T/{}^4T$  splitting is around 300 cm<sup>–1</sup> for Cu(OEP) and around 700 cm<sup>–1</sup> for Cu(TPP).<sup>78</sup> The emission from Cu(OEP) exhibits well-resolved vibronic structure, and the loss of the  $^2T$  origin is evident when the temperature is as low as 20 K.<sup>80</sup>

In contrast, Cu(TPP) gives a broad-band emission that shows only a hint of structure at low temperatures.<sup>78,81</sup> Antipas et al. reasoned that the spectral broadening was a result of the influence of a close-lying  $\pi^* \leftarrow d$  CT state.<sup>81</sup> As a test, they checked to see if the complex exhibited emission in a mixture of pyridine and THF, and they found none. The expectation was that the coordination of pyridine would lower the energy of the CT state and quench the emission entirely. They also cited Pariser–Parr–Pople calculations that were consistent with the existence of a relatively low-energy  $\pi^* \leftarrow d$  state.<sup>82</sup> However, X $\alpha$  calculations by Case and Karplus indicated that the low-lying CT state actually has  $d \leftarrow \pi$  character.<sup>83</sup>

## D. New Aspects of the Photochemistry

In 1988 two temperature-dependence studies appeared. Yan and Holten investigated the decay of the excited-state absorption spectra (ESA) of Cu(OEP) and Cu(TPP) as a function of temperature.<sup>84</sup> They found that the lifetime of photoexcited Cu(OEP) increased from 270 ns to 10  $\mu$ s in methylcyclohexane as the temperature ranged from 298 to 150 K. At the same time, the excited-state lifetime of Cu(TPP) remained essentially constant at 35 ns over a similar temperature range. They rationalized the data in terms of the participation of a thermally accessible CT state. In the case of Cu(OEP) the analysis suggested that the barrier to decay of the  $^{2,4}T$  system via the CT state was 600–800 cm<sup>–1</sup>. To explain the results with Cu(TPP), they proposed that the quenching state had an energy somewhere between that of the  $^2T$  and  $^4T$  states, very close to the  $^4T$  state. The

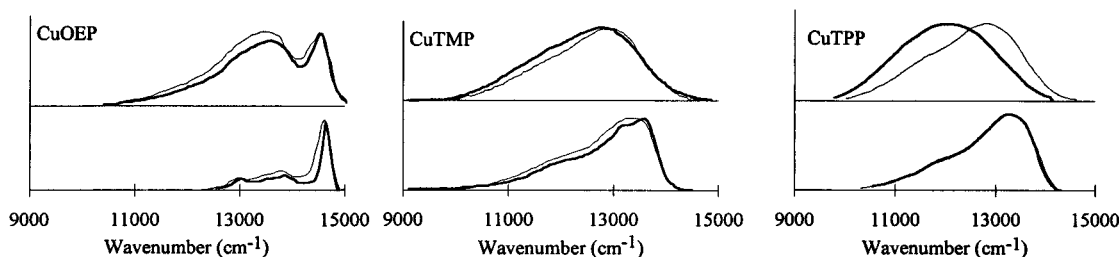


**Figure 7.** Emission spectra of Cu(OEP), Cu(TMP), and Cu(TPP) in toluene and a polymer matrix. The thin (thick) traces depict spectra obtained in the polymer (toluene); the top (bottom) spectra pertain to room temperature (77 K). (Reproduced with permission from ref 86. Copyright 1995 Elsevier Science S.A.)

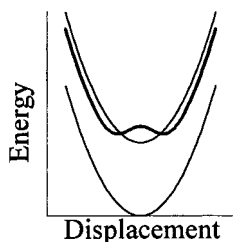


**Figure 8.** Schematic potential energy surfaces for a copper(II) porphyrin. The thick curve depicts an excited state that is subject to a vibronic distortion. The geometry change facilitates electronic to vibrational energy conversion and radiationless decay. The spin change may suppress the distortion in the  $^4T(a_{2u})$  state.

35 ns lifetime was then attributable to decay from the  $^2T$  state to the quenching CT state.<sup>84</sup> Within this model, the microsecond lifetimes obtained from Cu(TPP) in rigid matrices at low temperatures are explicable in terms of phosphorescence from the  $^4T$  state.<sup>80,85</sup> The assumption is that under these conditions the trip-quartet state does not deactivate via the higher-energy CT state. About the same time, Asano et al. focused on the emission spectra and formulated a quite different model.<sup>78,86</sup>

The model proposed by Asano et al. revolved around the temperature dependence of the band shape. Spectral studies of Cu(OEP) revealed a structured emission which occurred at essentially the same energy at all temperatures in toluene. Moreover, the complex gave virtually the same emission spectrum in a rigid polymer matrix (Figure 7). In the case of Cu(TPP) the emission showed some shift to lower energy in a poly(methyl methacrylate) matrix (PMMA) as the temperature dropped from 300 to 77 K (Figure 7). However, when the solvent was toluene, the shift was much greater. Curiously, at 77 K when both media were rigid, the two samples gave the same emission spectrum. The emission from the TMP complex was intermediate in character. The band shape was broad and poorly resolved like that of Cu(TPP), but the compound gave the same emission at any given temperature in both toluene and the polymer matrix. Asano et al. ascribed the broadening and part of the spectral shift exhibited by Cu(TPP) to a vibronic distortion within the emitting state. Figure 8 contains a schematic, double-minimum potential energy surface that illustrates the effect. In this model, thermal population of excited vibrational levels within the emitting state promotes deactivation. On the other hand, the presence of a rigid matrix tends to inhibit the distortion and enhance the lifetime. Indeed, some

time ago Gouterman and co-workers reported that the emission lifetime of Cu(TPP) increased to as long as a millisecond in a rigid polymer matrix at 25 K.<sup>80</sup> In light of the fact that a matrix like PMMA seemed to suppress the distortion, Asano et al. concluded that the motion involved some type of low-frequency out-of-plane nuclear motion, possibly involving a doming or ruffling of the porphyrin. They also noted that the emissions from systems with a relatively temperature-independent lifetime and a broad emission band shape generally involve excitation from the  $a_{2u}$  molecular orbital. They went on to suggest that the excited state in question might be especially prone to a doming distortion because the excitation shifts electron density away from the donor nitrogens to the C $\alpha$  and C $\beta$  carbons.<sup>78,86</sup> This model is appealing, but there are some unanswered questions: One obvious one is if the electronic excitation promotes doming, why is there no indication of a distortion in the spectrum of the palladium(II) analogue? After all, it entails a longer metal-to-nitrogen distance than Cu(TPP).<sup>87,88</sup> Thus, in contrast to the copper complex, the palladium derivative exhibits well-resolved vibrational structure, even at room temperature.<sup>89,90</sup>

To shed more light on the nature of the intermediate state involved in the radiationless decay scheme, Cunningham et al. carried out extensive physical studies on a series of copper(II) porphyrins.<sup>91</sup> Table 2 presents some of the data obtained. The electrochemical reduction potential for ring oxidation is of interest because this should be a major determinant of the energy of the lowest-energy ligand-to-metal CT state.<sup>92</sup> However, the data are clearly inconsistent with the notion that a thermally accessible CT state promotes deactivation. Thus, systems with relatively low reduction potentials, e.g., Cu(OEP) and Cu(TMP), exhibit some of the longer lifetimes in the series. It is just as evident that deactivation does not occur via a d–d excited-state either. Thus, the EPR parameters, like the  $g_{||}$  values in Table 2 reveal that the energies of the d–d excited states are practically constant in the series. Significant variations would have to exist if deactivation through a d–d state were to explain the lifetime data. Besides, theory suggests that the d–d states are thermally inaccessible with energies of  $\sim 20\,000\text{ cm}^{-1}$ .<sup>93</sup>

By process of elimination, the model that invokes a vibronic distortion within the  $^2,4T(a_{2u})$  system seems most likely to explain the photophysics of compounds such as Cu(TPP). Asano-Someda et al. proposed a ruffling or doming distortion.<sup>86</sup> A doming distortion would be more consistent with Cu–N bond elonga-

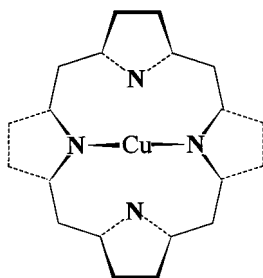


**Figure 9.** Extreme example of a sitting-atop distortion. Vibronically induced mixing with a ligand-to-metal CT state could promote this type of distortion in a  $\pi-\pi^*$  excited state of Cu(TPP).

tion, and this could also account for the influence of the mesityl groups of Cu(TMP) on the excited-state lifetime, as mesityl substituents reportedly inhibit ring doming.<sup>94</sup> Still, the question remains as to why the distortion is unique to copper porphyrins. In view of the fact that the hallmark of copper is the stability of the copper(I) state, it is possible that the emitting state takes on an admixture of CT character in conjunction with a vibronic distortion.<sup>91</sup> If so, the distortion is likely to involve the formation of some type of sitting-atop structure in accordance with the ionic radius of copper(I). In one possible configuration, the metal moves out of the mean plane of the porphyrin along with two of the ring nitrogens so as to preserve two relatively short metal–nitrogen bonds (Figure 9).<sup>95,96</sup> The attractive feature of this model is a recognition of the legitimate role that the  $d^{10}$  configuration can play in the photophysics even if the CT states themselves are thermally inaccessible. There is a report of the observation of a CT excited state in the time-resolved resonance Raman spectrum of Cu(TPP).<sup>97</sup> Detection of the thermally populated  $^2T$  state is an alternative possibility as the separation of this state from the trip-quartet state may vary with the distortion. Indeed, if vibronic forces induce an admixture of CT character, the mixing is apt to be more important in the  $^2T$  state because of its doublet character. This could give rise to a well structure like that in Figure 8. The existence of multiple conformations of the excited state in solution could also account for the complexity of the spectrum.<sup>98</sup>

## E. Exciplex Formation

Coordinating solvents deactivate photoexcited copper(II) porphyrins, and most workers assume that a CT excited state has a role in the process. Early on, Antipas et al. reasoned that the energy would funnel out of the  $\pi^* \leftarrow d$  excited state when it dropped below the emitting  $\pi-\pi^*$  state as a result of the addition of an axial ligand.<sup>81</sup> Later, Kim et al. cited calculations which indicated that a similar effect can occur with a  $d \leftarrow \pi$  state when the core of the porphyrin expands and the metal moves out of the plane toward an axial ligand.<sup>99</sup> Kim et al.'s report about the influence of a fifth ligand led Hudson et al. to investigate the binding interactions of Cu(T4) with DNA by luminescence methods.<sup>100</sup>

Later studies employed Stern–Volmer methods to study the emission quenching of neutral porphyrin

**Table 3.** Rate Constants for Quenching in Toluene at 25 °C

quencher	$k_q, M^{-1} s^{-1}$	
	Cu(TPP)	Cu(TMP)
pyridine	$2.3 \times 10^9$	$1.1 \times 10^8$
2-methylpyridine	$1.7 \times 10^9$	$7.7 \times 10^8$
2,6-dimethylpyridine	$2.3 \times 10^6$	$6 \times 10^5$

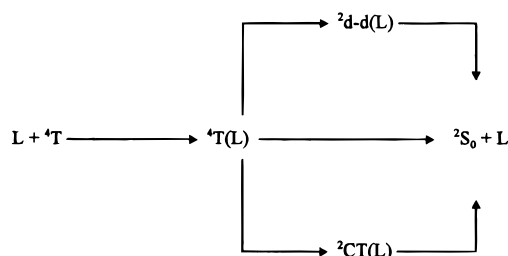
complexes by a series of Lewis bases in the noncoordinating solvent toluene.<sup>101</sup> Consistent with an associative mechanism, the quenching constant increases with the donor strength (Figure 4). For example, in the case of Cu(TMP) the quenching rate constant increases from  $4.0 \times 10^8 M^{-1} s^{-1}$  for acetonitrile to  $2.3 \times 10^9 M^{-1} s^{-1}$  for pyridine. Pyridine is the stronger base and has a Gutmann donor number of 33.1 compared to 14.1 for acetonitrile.<sup>102</sup> Systematic studies of steric effects are also in accord with a quenching mechanism that entails the attack of a fifth ligand. Thus, the data in Table 3 reveal that the addition of sterically active methyl groups on either the base or the copper porphyrin inhibit quenching. The temperature dependence of quenching is also relevant because if reversible exciplex formation occurs, the enthalpy of activation for quenching can be quite small or even negative.<sup>41</sup> In fact, the results showed that  $\Delta H_q^\ddagger \approx 2 \text{ kJ mol}^{-1}$  for weak donors such as acetonitrile and about 11 kJ mol<sup>-1</sup> for the stronger donor DMSO.<sup>101</sup> The small positive activation enthalpy observed for acetonitrile is in accord with the proposed exciplex quenching pathway.

Parallel Raman studies by Apanasevich et al. have contributed a great deal of insight into the solvent-induced quenching phenomenon.<sup>103</sup> Their ESA results showed that strong donors such as pyridine rapidly quench the excited state of Cu(OEP). In the case of pyridine, the lifetime is about 80 ps, and they attributed the decay to deactivation via a low-energy CT state of the five-coordinate adduct. However, with THF as a quencher, they observed a biphasic decay. The shorter of the two lifetimes was 140 ps, and they associated this with the loss of the  $\pi-\pi^*$  excited state. The second process, which had a lifetime of 360 ps, corresponded to the decay of a successor complex. On the basis of the excitation profile of the transient Raman spectrum, they proposed that the successor complex was a five-coordinate,  $d-d$  excited-state species, more specifically, a  $z^2 \rightarrow x^2-y^2$  state.<sup>103</sup> Population of the sigma-antibonding  $d(x^2-y^2)$  orbital encourages an expansion of the porphyrin core and/or movement of the metal center out of the plane of the ligand. The decreases in the frequencies of the porphyrin core marker transitions listed in Table 4 support this interpretation. For comparison, Table 4 also contains some data for Ni(OEP). Note the shifts in frequency of the  $\nu_2$  and  $\nu_4$  vibrations that occur as a result of excitation from the  $^1S_0$  ground state to the  $^3B_{1g}(z^2 \rightarrow x^2-y^2)$  excited state. A similar effect occurs with Cu(OEP) upon the promotion of a second electron to the  $x^2-y^2$  orbital and the addition of the THF ligand (Table 4). Apanasevich et al. interpreted the results with a variation of Scheme 2.

**Table 4. Raman Bands (cm<sup>-1</sup>) from the Ground ( $\nu$ ) and Excited ( $\nu^*$ ) States of Metalloporphyrins in Different Media**

mode	motion	Ni(OEP) <sup>a,b</sup>	Cu(OEP) <sup>b</sup>		Cu(TPP) <sup>c</sup>		Cu(T4) <sup>d</sup>	
		THF	PhH	THF	PhH	THF	buffer	w/[poly(dA-dT)] <sub>2</sub>
$\nu_2$	$C_\beta-C_\beta$	1604	1593	1594	1563	1565	1571	1571
$\nu^*_2$		1581		1584		1543	1553	1552
$\nu_3$	$C_\alpha-C_M + C_\beta-C_\beta$	1519	1504	1504	1458	1452		
$\nu^*_3$		1494		1491		1448		
$\nu_4$	$C_\alpha-N + C_\alpha-C_\beta$	1383	1380	1379	1364	1366	1367	1366
$\nu^*_4$		1375		1365		1342	1347	1348

<sup>a</sup> <sup>3</sup>B<sub>lg</sub>(d-d) state. <sup>b</sup> Apanasevich, P. A.; Chirvony, V. S.; Kruglik, S. G.; Kvach, V. V.; Orlovich, V. A. In *Laser Applications in Life Sciences*; Akhmanov, S. A., Poroshina, M. Y., Eds.; Proceedings of SPIE, Vol. 1403, Part I; SPIE: Bellingham, WA, 1991; pp 195–211. <sup>c</sup> Kruglik, S. G.; Apanasevich, P. A.; Chirvony, V. S.; Kvach, V. V.; Orlovich, V. A. *J. Phys. Chem.* **1995**, *99*, 2978–2995. <sup>d</sup> Kruglik, S. G.; Ermolenkov, V. V.; Shvedko, A. G.; Orlovich, V. A.; Galievsky, V. A.; Chirvony, V. S.; Otto, C.; Turpin, P. Y. *Chem. Phys. Lett.* **1997**, *270*, 293–298.

**Scheme 2**

In this scheme  $^2S_0$  denotes the four-coordinate ground state, L denotes a weak oxygen donor, such as THF, T(L) denotes an exciplex of the  $\pi-\pi^*$  excited state, d-d(L) denotes a second exciplex of the d-d excited state, and CT(L) denotes the ever popular, but as yet undetected, five-coordinate CT state. The justification for invoking the CT(L) state was the inability to saturate the d-d(L) excited state even at very high laser intensities.<sup>103,104</sup> However, if T(L) branches to the ground state as well as the d-d(L) state, it is possible to rationalize the power dependence without invoking the CT(L) state. Other groups have also used Raman techniques to study these systems.<sup>97,105</sup>

There are also some recent studies of the water-soluble Cu(T4) system available. Jeoung et al. monitored the EAS spectrum in aqueous solution and reported finding transients with lifetimes of 3.2 and 11.9 ps.<sup>106</sup> They also analyzed a shoulder that appeared on the low-frequency site of the  $\nu_2$  band in the transient Raman spectrum, and they ascribed this to overlapping signals from two excited states. Kruglik et al. later confirmed the  $15 \pm 5$  ps transient, but the second component they detected had a relatively long lifetime,  $\tau_2 \gg 1$  ns.<sup>107</sup> They assigned the transient Raman signals to the latter component which they identified as a d-d excited state with an axially bound water. They rationalized the low yield ( $\phi \leq 0.1$ ) of the d-d excited-state adduct in terms of competitive deactivation via a five-coordinate CT state. However, as noted above, direct decay of the five-coordinate  $^{2,4}\pi-\pi^*$  state would be another possibility.

To summarize this section on exciplex quenching, various authors have invoked at least three different types of exciplexes, any of which decay to yet another five-coordinate form that is in the ground electronic state. The Raman studies provide good evidence for

the existence of a five-coordinate d-d state. As it is the precursor, the five-coordinate  $\pi-\pi^*$  state must also exist, either as an intermediate or a transition state. The notion that a five-coordinate CT state plays the pivotal role in the decay remains popular, but, so far, has little in the way of experimental support.

**V. Copper Porphyrins and DNA****A. Binding Interactions**

Over a period of years, work from several laboratories has established that cationic metalloporphyrins utilize three fundamentally distinct modes of binding to DNA.<sup>68,108,109</sup> For present purposes the intercalative and external, or groove, binding modes are of particular interest. In a third type of adduct, porphyrin ions stack atop each other (aggregate) along the DNA double helix and give a strong conservative CD signal in the Soret region as a characteristic spectroscopic signature.<sup>108,110</sup> Table 5 summarizes the physical attributes of the other two types of adducts, and Figure 10 provides schematic representations of the various forms. As Table 5 indicates, strong hypochromism in the Soret region is a telltale sign of intercalation as is an induced CD signal with a negative amplitude.<sup>108,111</sup> Furthermore, flow dichroism studies show that in this type of adduct the plane of the porphyrin is roughly orthogonal to the helix axis.<sup>112</sup> Due to the elongation and/or rigidification of the DNA molecules in solution, intercalation also causes an increase in the specific viscosity.<sup>113</sup> Another indication is the downfield shift of a peak in the <sup>31</sup>P NMR spectrum of the duplex.<sup>109,114</sup> Only free porphyrins, like H<sub>2</sub>T4, or a metalloporphyrin without axial ligands, like Cu(T4) or Pd(T4), is capable of intercalating into DNA, but these systems can undergo groove binding as well.<sup>68,108,109</sup> Groove binding, but not intercalation, is possible when the metalloporphyrin has an axial ligand, like Zn(T4) which

**Table 5. Characteristics of DNA Adducts of Cu(T4)**

property	groove binding	intercalation
Soret shift, nm	-4	-10
% H	$\pm 5$	30
CD (Soret)	$\Delta\epsilon > 0$	$\Delta\epsilon < 0$
$^{2,4}\pi-\pi^*$ emission	weak	large enhancement
$\eta/\eta_0$	—	increase 50%
<sup>31</sup> P NMR	some broadening	downfield peak

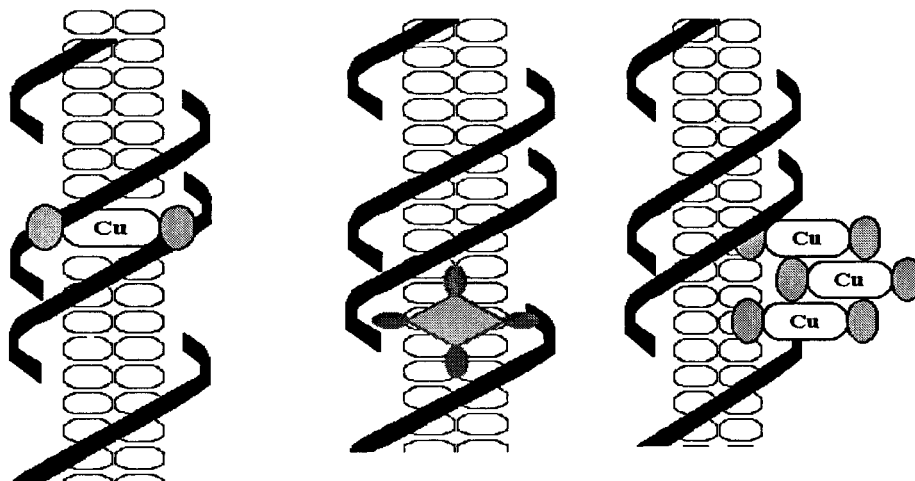


**Figure 10.** Schematic views of different binding modes involving double helical DNA and a porphyrin substrate. From the left, B-form DNA with intercalated Cu(T4) having two of its pyridyl substituents in the minor groove, with Cu(T4) oriented face on in the major groove, and with outside stacking of the porphyrin.

exists as a monosolvate complex in solution.<sup>111,115</sup> A groove-bound adduct exhibits modest hypochromism or even an absorbance increase at the Soret maximum. In contrast to intercalation, groove binding typically induces a positive CD signal and has little influence on the specific viscosity. Finally, there are relatively small perturbations in the NMR spectrum.<sup>109</sup> Flow dichroism studies reveal that the porphyrin plane makes an angle of about 65° with the helix axis in the case of Zn(T4)<sup>112</sup> and about 45° in the case of the cobalt(III) analogue,<sup>116</sup> both of which are groove binders.

## B. Specificity

Groove binders show a preference for interacting in regions rich in A=T base pairs. With only two hydrogen bonds connecting the base pairs, it is possible that AT-rich structures melt readily and permit optimization of the contacts with the porphyrin ligand.<sup>117</sup> In contrast, intercalators seek out GC-rich regions of DNA. Footprinting studies illustrate these trends. Thus, groove-binding M(T4) species protect AT-rich areas of DNA, e.g., when M = Mn, Fe, Co, or Zn.<sup>118</sup> On the other hand, Ni(T4) and Cu(T4), which are capable of intercalation, protect GC-rich as well as AT-rich domains.<sup>118</sup> Other footprinting studies suggest that a CpG or a TpA step frequently occurs at the center or near a site protected by the binding of H<sub>2</sub>T4 or Ni(T4).<sup>119</sup> Some time ago, Marzilli and co-workers carried out NMR studies which suggested that H<sub>2</sub>T4 intercalates highly specifically within a 5'CG3' step, although there is evidence of parallel groove binding.<sup>109,120</sup> However, subsequent studies have shown that the free ligand intercalates into poly(dA-dC)·poly(dG-dT) as well which, of course, has no 5'CG3' steps.<sup>121</sup> In later studies Marzilli and co-workers have found that Ni(T4) is not as selective as H<sub>2</sub>T4 and does not require a 5'CG3' step for intercalation to occur.<sup>114</sup> In the case of Cu(T4) Dougherty and Pasternack have used EPR to monitor the binding and have concluded that the complex intercalates preferentially between adjacent G=C base pairs but that the particular base sequence is not crucial.<sup>122</sup>

## C. Structure of the Adducts

The structure of the intercalated adduct has always seemed more or less self-evident. Early on, Fiel and Munson proposed that the porphyrin sandwiches between two base pairs so that two of the pyridinium substituents are in the minor groove and two are in the major groove.<sup>123</sup> Calculations by Hui et al. were consistent with this picture.<sup>124</sup> A later analysis of ENDOR data by Greiner et al. predicted partial intercalation of Cu(T4).<sup>125</sup> They concluded that the copper center did not reside on the helix axis and that the porphyrin extended into the major groove. Finally, in 1996 Williams and co-workers published the crystal structure of a 2:1 adduct of Cu(T4) with [d(CGATCG)]<sub>2</sub>, and there were some surprises.<sup>12</sup> In this structure the Cu(T4) ions do lodge within the 5'CG3' steps, but there is a partial unraveling at each end of the duplex. As a result the cytidine bases flip out away from the original stack of base pairs (Figure 11). However, the base pairing is complete because the terminal G's on each strand pair with C's that extend over from neighboring duplexes in the crystal lattice. For each porphyrin, two of the pyridinium substituents reside in the minor groove near phosphate groups, and two rest in the major groove. Steric interactions involving the pyridinium groups provide the impetus for a significant extension of each helix. In fact, almost all of the van der Waals contacts involve atoms of the substituent groups and the sugar-phosphate backbone. Williams and co-workers term this unusual mode of binding "hemi-intercalation". In view of the steric forces involved, they propose that intercalation will result in a flipped-out base in solution as well.

The ideas concerning the local structure about externally bound H<sub>2</sub>T4 or any of its metal-containing derivatives are much less definite. As noted above, flow dichroism measurements indicate that the plane of the porphyrin is neither parallel nor perpendicular to the helix axis, but canted. Largely on the basis of DNA-cutting experiments, one hypothesis is that the porphyrin binds edge on along the minor groove.<sup>68,116,126</sup> The canonical structure of DNA may, however, be irrelevant if appreciable melting of the local structure

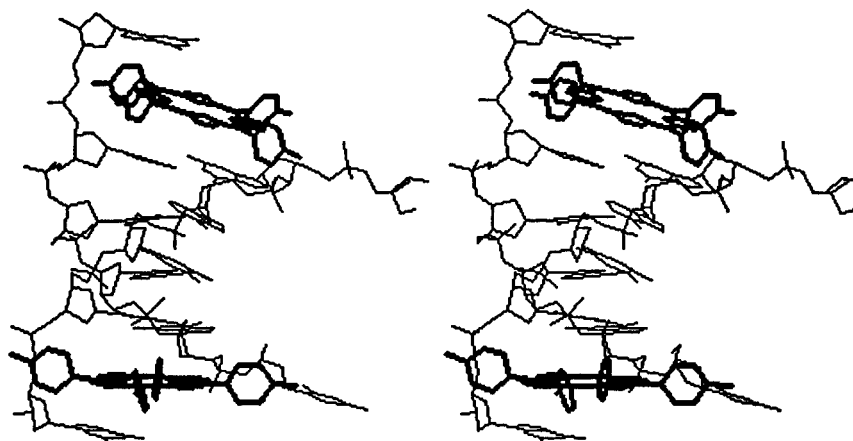


**Figure 11.** Stereodrawing of the structure reported for Cu(T4) bound to  $[d(CGATCG)]_2$  in the crystalline state.<sup>12</sup> Note that the porphyrin inserts in the 5'CG3' step but that fraying occurs and the terminal C's intrude into a neighboring duplex.

**Table 6. Physical Data for Cu(T4) at DNA-P/Cu = 100, pH 7.8, and 25 °C<sup>a</sup>**

type of DNA	% G≡C	$\lambda_{\text{max}}^{\text{abs}}$ , nm <sup>b</sup>	$\phi_{\text{rel}}^c$	$\tau$ , ns
[poly(dG-dC)] <sub>2</sub>	100	439	100	22
<i>M. luteus</i>	73	439	73	21
ST	41	428	34	18
<i>Cl. perfringens</i>	27	428	26	19
[poly(dA-dT)] <sub>2</sub>	0	428		

<sup>a</sup> Hudson, B. P.; Sou, J.; Berger, D. J.; McMillin, D. R. *J. Am. Chem. Soc.* **1992**, *114*, 8997–9002. <sup>b</sup> Absorbance maximum occurs at 425 nm in the control. <sup>c</sup> Estimated uncertainty  $\pm 10\%$ .

occurs. External binding may induce kinking of the DNA as well, because it is more difficult to orient DNA molecules in the presence of groove binders.<sup>116</sup> An alternative to edge-on binding is face-on binding within the major groove.<sup>109</sup>

## D. Luminescence Studies

In view of the influence axial ligands have, luminescence techniques are useful for probing the DNA-binding interactions of Cu(T4).<sup>100</sup> The original hope was that it would be possible to observe emission from the intercalated form of the complex, and this proved to be the case. In aqueous solution Cu(T4) gives virtually no detectable emission signal due to solvent-induced quenching, but upon addition of ST DNA, a signal appears. The signal is broad-band, much like the one from Cu(TPP) in a nondonor solvent like toluene. The same comparison is apropos for the emission intensity ( $\phi \approx 10^{-4}$ ) and the lifetime ( $\tau \approx 20$  ns) of the DNA adduct. At a phosphate-to-copper ratio (DNA-P/Cu) of 50 with ST DNA, uptake is complete, but more than one type of bound porphyrin is present. This is evident from the fact that the absorbance maximum of the Soret band occurs at 428 nm, while the maximum in the excitation spectrum occurs at  $\sim 438$  nm. Table 6 summarizes some of the physical data taken at DNA-P/Cu = 50 for different types of DNA. The DNA that is rich in G≡C base pairs, like *M. luteus* or [poly(dG-dC)]<sub>2</sub>, yields an emissive adduct that exhibits absorption and excitation maxima at  $\sim 438$  nm. In addition, these adducts exhibit a negative CD signal in the

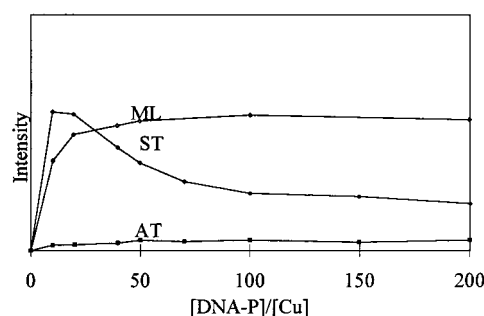


**Figure 12.** Emission intensity from Cu(T4) as a function of the DNA-P/Cu ratio for samples with different percentages of G≡C base pairs.<sup>100</sup> ML is *M. luteus* DNA (73%), ST is salmon testes DNA (41%) and AT is [poly(dA-dT)]<sub>2</sub>.

Soret region, consistent with intercalative binding. In contrast, the adduct with [poly(dA-dT)]<sub>2</sub> exhibits practically no emission and has its absorbance maximum around 428 nm. As noted above and in line with groove binding, the induced CD signal is positive in the presence of [poly(dA-dT)]<sub>2</sub>.<sup>68,108,109</sup> In general, the intensity of the emission signal increases with the proportion of G≡C base pairs present in the DNA. In the case of ST DNA both types of binding clearly occur. The groove-bound fraction dominantly influences the absorbance spectrum, but the intercalated form is mainly responsible for the emission intensity. Hence, the excitation maximum occurs around 438 nm.

The CD results as well as the emission data in Figure 12 reveal that the nature of the binding interaction can vary in a complicated way with the nucleotide-to-porphyrin ratio. The emission data for *M. luteus* DNA are consistent with intercalation as the dominant type of binding interaction and saturation at high DNA-P/Cu ratios. Some degree of groove binding may occur as well, but it has to be a minor effect. On the other hand, in the case of [poly(dA-dT)]<sub>2</sub>, groove binding dominates. (In this case the CD results suggest outside stacking occurs at low DNA-P/Cu ratios;<sup>100</sup> if so, the outside-stacked form must be virtually nonemitting.) Of all the systems shown in Figure 12 the behavior with ST DNA is the most interesting in that the emission intensity rises to a maximum around DNA-P/Cu = 10. With the addition of more DNA, the emission drops off and finally

**Table 7. Data for Hairpin Adducts of Cu(T4)<sup>a</sup>**

hairpin	label	$\lambda_{\text{max}}^{\text{ABS}}$ , nm	% H <sup>b</sup>	CD		$\Phi_{\text{rel}}^d$
				$\lambda_{\text{max}}$ , nm	$\Delta\epsilon^c$ M <sup>-1</sup> cm <sup>-1</sup>	
AT-Rich Stems						
<b>GATAAC</b> <sup>T</sup> <sub>T</sub> CTATTG <sup>T</sup> <sub>T</sub>	TA	427	$-2 \pm 2$	421	17	0.1
<b>CATAAG</b> <sup>T</sup> <sub>T</sub> GTATTC <sup>T</sup> <sub>T</sub>	TA*	429	$-5 \pm 2$	421	9	0.2
<b>GAATAC</b> <sup>T</sup> <sub>T</sub> CTTATG <sup>T</sup> <sub>T</sub>	AT	428	$5 \pm 2$	415	$5 \pm 1$	0.2
<b>CAATAG</b> <sup>T</sup> <sub>T</sub> GTTATC <sup>T</sup> <sub>T</sub>	AT*	429	10	422	7	0.2
<b>AGATAC</b> <sup>T</sup> <sub>T</sub> TCTATG <sup>T</sup> <sub>T</sub>	AT'	429	10	413	$5 \pm 1$	0.2
GC-Rich Stems						
<b>GAGCAC</b> <sup>T</sup> <sub>T</sub> CTCGTG <sup>T</sup> <sub>T</sub>	GC	432	20	433	-22	1.0
<b>GACGAC</b> <sup>T</sup> <sub>T</sub> CTGCTG <sup>T</sup> <sub>T</sub>	CG	434	25	434	-27	0.9
<b>GAGAAC</b> <sup>T</sup> <sub>T</sub> CTCTTG <sup>T</sup> <sub>T</sub>	GA	432	20	435	-22	0.7
<b>GACAAC</b> <sup>T</sup> <sub>T</sub> CTGTTG <sup>T</sup> <sub>T</sub>	CA	432	20	434	-17	0.5

<sup>a</sup> Hairpin-to-copper ratio of 5. <sup>b</sup> % H expresses the percent change in absorbance at the Soret maximum. <sup>c</sup> Error  $\pm 2$  unless otherwise noted. <sup>d</sup> Error  $\pm 0.1$ .

plateaus at a lower intensity. Similar changes occur in the absorption spectrum. Thus, at lower DNA-P/Cu ratios there is a strong red shift and significant hypochromism in the Soret region, while at higher ratios the absorption band shifts back toward shorter wavelength and the absorption intensity returns.<sup>100</sup> Independent of the DNA-P/Cu ratio, however, the emission excitation maximum remains at 438 nm. These data indicate that the intercalative mode of binding is more competitive at moderately high loadings of porphyrin but that the complex shifts to external sites when the DNA is in excess. Data reported by Carvlin and Fiel are also consistent with this model.<sup>127</sup> Hudson et al. interpreted this to mean that the groove-bound form of the porphyrin has a larger footprint than the intercalated form.<sup>100</sup> In this view intercalative binding is strongly favored over groove binding at moderate loads of porphyrin, when DNA is the limiting reagent. However, when excess DNA is present, there is no problem with interference from other porphyrins in neighboring groove sites, and a redistribution of the ligand occurs. The drop in the emission intensity results from a reduction in the proportion of intercalated Cu(T4). Evidence for a redistribution among binding sites, or a load-dependent structural reorganization, were also apparent in a titration with [poly(dG-dC)]<sub>2</sub>.<sup>100</sup>

Because the groove-bound form is essentially non-emissive, luminescence methods reveal information about the intercalated form of Cu(T4). In the externally bound form, the axial coordination sites of the copper are accessible, and the attack of a fifth ligand quenches the excited state. At present, the exact identity of the quencher is still an open question. Hudson et al. have proposed that a solvent molecule

is the likely culprit.<sup>100</sup> In accordance with this hypothesis, there are indications that metalloporphyrins with axially coordinated solvent molecules can reside in groove-binding sites.<sup>116</sup> However, other investigators have proposed that the attacking group is a donor atom on the surface of the DNA molecule, vide infra. Luminescence studies have provided further evidence that guanine-cytosine base pairs promote intercalation and adenine-thymine base pairs promote groove binding. The luminescence data have also provided new information about how the distribution among binding sites varies with the loading. These same techniques can also provide information about binding specificity, but that requires the use of substrates other than random-sequence samples of DNA or long-chain alternating polymers.

### E. Hairpin Hosts

As a means of getting at the base dependence of the DNA-binding interactions, hairpin, or stem-loop, structures are useful hosts. Hairpin-forming oligonucleotides are convenient sources of short segments of B-form DNA because they are stable at micromolar concentrations. Eggleston et al. have used 16-mers that have a T<sub>4</sub> loop and a stem end six base pairs long.<sup>128</sup> Concentration-dependent melting profiles confirm that in every case the hairpin conformation is the dominant conformation in solution. Table 7 summarizes some representative data and gives the compositions of the relevant hosts as well as the explanation of the shorthand names. Because the mode of binding is quite sensitive to the base sequence in the stem region, loop binding does not appear to be a competitive process under the condi-

tions used. All of the data reported pertain to an oligonucleotide-to-copper ratio of 5 which is more than sufficient to ensure complete uptake. As discussed below, it is possible to divide the hairpins into two classes according to the percentage of G≡C base pairs in the stem. Note that each hairpin has at least two G≡C base pairs, one at either end of the stem, to minimize fraying.

The class I hairpins have the AT-rich stems and appear at the top of Table 7, while the class II hairpins have GC-rich stems. The spectral data reveal that the adducts of the class I hairpins all involve external binding. Thus, with these systems the bound porphyrin exhibits a small red shift in the Soret absorption, modest hypochromism or even hyperchromism at the absorption maximum, a positive CD signal and weak emission. The TA and the TA\* hairpins give the CD signal of archetypical groove-bound Cu(T4). However, for the AT and AT\* hosts the CD signals in the Soret region are weaker, although still positive. Competitive formation of two types of adducts with opposing CD signals could account for the reduced intensity, but this is doubtful because the emission excitation signal matches the absorption maximum in all cases. In all probability the CD results simply reflect the fact that different sequences support different types of groove adducts, consistent with an "induced-fit" mode of binding.<sup>128</sup> (For the groove-bound adducts, the CD maximum falls at a shorter wavelength than the absorption maximum. In principle, this could be due to a reduction of symmetry and a splitting of the orbitally degenerate  $E_u$  excited state. However, the Soret band actually narrows upon formation of the groove-bound adduct.) Class II hairpins have three or four G≡C base pairs in the stem (Table 7). With these hosts the porphyrin adducts exhibit a strong red shift in the Soret maximum, hypochromism, a negative CD signal, and a relatively strong emission signal. These are all classic signs of intercalation.

The results with the hairpin hosts provide important information about the binding preferences. For example, the data show that runs of four A=T base pairs in a segment six base pairs long suffice to define a groove-binding site for Cu(T4). However, more than one type of binding occurs depending on the sequence. The footprint of intercalative binding is probably smaller and may contain only a single G≡C base pair as long as the double helix is relatively rigid in that location. Although the spectral data obtained provide no direct information about the site of intercalation, the hypochromism is consistent with intercalation next to a G≡C base pair or between contiguous G≡C base pairs. NMR studies will provide more specific structural information. Finally, the data suggest that hemiintercalation may not be an important phenomenon in solution. The fact that both the AT and the AT' hairpins form external adducts is the basis of this assertion. If hemiintercalation were a favorable mode of interaction, one would expect it to occur with the AT' host. One reason is that this host does not have a run of four A=T base pairs in the stem. Second, of all the systems in Table 7, base expulsion should occur most

readily at the stem terminus of the AT' hairpin. Yet, AT' gives a typical groove-bound adduct no different from that of AT. It is possible that the AT, AT\*, and AT' systems all support hemiintercalation. If so, this is a very different type of adduct than one finds with GC-rich types of DNA. Clearly, more work will be necessary to clarify the modes of binding in detail.

## F. Transient Raman Studies

Raman techniques have provided some very important information about an exciplex derived from the groove-bound Cu(T4). Early studies utilizing continuous wave laser sources showed that the interaction with [poly(dG-dC)]<sub>2</sub> perturbs a band in the Raman spectrum of the Cu(T4) chromophore at 1100 cm<sup>-1</sup>. This band corresponds to a  $\delta(C_\beta-H)$  deformation, and the shift suggests that intercalative binding may perturb the dihedral angle that the pyridine substituent makes with the plane of the porphyrin.<sup>129a</sup> In contrast, the same peak shows almost no shift when [poly(dA-dT)]<sub>2</sub> is the host. In time-resolved studies reported in 1990, Nakamoto and co-workers observed two new Raman-scattering peaks in a resonance Raman spectrum of the adduct of Cu(T4) with DNA or [poly(dA-dT)]<sub>2</sub>, but not [poly(dG-dC)]<sub>2</sub>.<sup>129b</sup> The peaks relate to a transient generated by laser excitation in the Soret region and are only observable with high-powered, pulsed-laser excitation. For reference, the resonance-enhanced ground-state spectrum of Cu(T4) contains the  $\nu_2$  core vibration at 1571 cm<sup>-1</sup> (mainly  $C_\beta-C_\beta$  stretching) and the  $\nu_4$  band at 1367 cm<sup>-1</sup> (mainly  $C_\alpha-N$  stretching). In the original article, the authors assigned the bands at 1552 and 1348 cm<sup>-1</sup> in the transient Raman spectrum to the same two vibrations on frequency grounds.<sup>129b</sup> Moreover, in view of the downshift in frequencies, they attributed the peaks to an exciplex with Cu(T4)<sup>+</sup>/dT<sup>-</sup> character. They reasoned that the loss of an electron would decrease the  $\pi$  bond order of the porphyrin and that a thymine residue would be the best acceptor. A subsequent study by Chinsky et al. utilized a two-color method.<sup>130</sup> Their results showed that the transient had a lifetime of much less than 20 ns and that the excitation maximum occurred only a few nanometers to the red of the ground-state adduct. They concluded that the transient might be some type of metastable ground-state adduct. A 1992 report by Nakamoto and co-workers provided data for several different types of DNA.<sup>131</sup> In particular, they found a very strong signal from the transient when the host was [poly(dA-dT)]<sub>2</sub> but a weak one when the host was poly(dA)·poly(dT). In studies involving oligonucleotides, they found that the transient only appeared with appreciable intensity when there was a run of four consecutive A=T base pairs (Figure 13). They attributed this to face-on binding of Cu(T4) in the major groove. They also found that the transient appeared in the spectrum obtained with a 32-mer that contained all G or C bases except for a central ATAT run. However, the intensity of the transient signal was power dependent, which they explained in terms of a photoinduced migration of Cu(T4) from intercalation to groove sites. An alternative possibility would be a temperature-



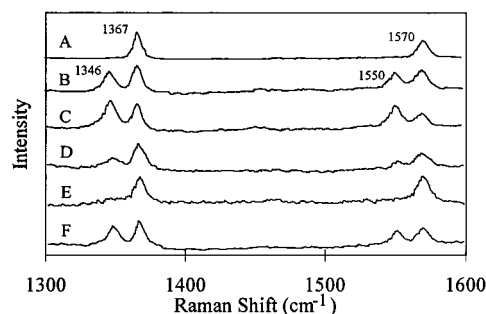


**Figure 13.** Resonance Raman spectra of Cu(T4) bound to various types of DNA. Except for spectrum A, the excitation source was a high-power, pulsed laser operating at 416 nm. Raman spectra of Cu(T4) with (A) calf thymus DNA (ground state only), (B) calf thymus DNA again, (C) [poly(dA-dT)]<sub>2</sub>, (D) poly(dA)·poly(dT), (E) [poly(dG-dC)]<sub>2</sub>, and (F) [d(GCGCGCATATGCGCGC)]<sub>2</sub>. (Reproduced with permission from ref 131. Copyright 1992 American Chemical Society.)

induced redistribution of Cu(T4) among binding sites as absorption-induced heating seems likely to occur. That same year, the model proposed by Hudson et al. to explain luminescence-quenching results suggested another model for the exciplex, namely a five-coordinate d-d state.<sup>100</sup>

Later investigations of transient Raman data adopt this explanation for the exciplex. In a 1993 paper, Turpin and co-workers reported that a similar transient occurs with poly(dT) or poly(rU) as a host.<sup>132</sup> On the basis of the Raman excitation profile and a comparison of the frequency shifts of the exciplex with those of the four- and six-coordinate forms of Ni(T4), they concluded that the shifts were consistent with expansion of the coordination number of copper and single occupancy of the d(z<sup>2</sup>) orbital. In light of these results and analogies with earlier studies,<sup>103,104</sup> they proposed that adduct formation may involve coordination of a carbonyl oxygen of the C2 or C4 carbons of a thymine residue. Coordination of an oxygen donor seems likely since this gives rise to a relatively long-lived exciplex with porphyrins such as Cu(OEP).<sup>103,104</sup> In their next report on the DNA adducts, they resolved the decay of the excited-state absorption of the adduct of Cu(T4) with [poly(dA-dT)]<sub>2</sub> into two phases.<sup>133</sup> The faster component exhibited a lifetime of 35 ± 7 ps, and the lifetime of the second phase was 3.2 ± 0.5 ns. They assigned these to the <sup>4</sup>T state and the exciplex, respectively. In contrast to other systems, they also noted that formation of the exciplex was a fairly high quantum yield process on the DNA support. At this juncture they posited a 21 ps decay for Cu(T4) in the absence of DNA and found no evidence for a nanosecond-lived exciplex involving bound water. As noted above, Jeoung and co-workers recently claimed to have detected an aquo form of the exciplex in studies with a laser system that utilizes 70 ps pulses.<sup>106</sup> They also found a 1.3 ps rise time in the ESA spectrum of the adduct with [poly(dG-dC)]<sub>2</sub>. They attribute this to the conversion from a five-coordinate form to the intercalated form.<sup>106</sup> However, since the favored geometry of the intercalated adduct may differ with the electronic configuration, it is possible that the spectral change corresponds to simple structural relaxation of the

intercalated complex. A subsequent paper by Kruglik et al. reported that the exciplex involving a bound water molecule forms in low yield and has a lifetime in excess of a nanosecond.<sup>107</sup> They also concluded that the adduct exhibits a distinctive blue shift in its Soret band.

## G. Summary

Many investigators continue to invoke a role for a CT excited state in the deactivation of photoexcited copper(II) porphyrins, but the experimental evidence in favor of the hypothesis remains very slim. Indeed, recent studies of substituent effects indicate that the nonradiative decay process does not depend on the population of a CT excited state. The emissive  $\pi-\pi^*$  state may, however, take on an admixture of CT character in conjunction with the vibronic distortion that facilitates relaxation. In the presence of a weak Lewis base, like THF, transient Raman data show that the formation of a five-coordinate d-d excited state occurs, but there is no sign of a corresponding exciplex involving a CT excited state.

The cationic complex Cu(T4) binds to random sequence DNA as a monomer via at least two distinct mechanisms. Intercalative binding requires the presence of G≡C base pairs, but they need not occur in succession. In aqueous solution, Cu(T4) is ordinarily nonemissive, but it exhibits luminescence when it intercalates into DNA. Water quenches the emission via formation of an exciplex, but intercalation into DNA blocks access to the axial coordination sites. A recent X-ray structure raises the possibility that Cu(T4) binds by a hemiintercalation mechanism which involves a flipped-out base.<sup>12</sup> It is, however, not clear that the same type of binding occurs in solution. A local composition of 50% G≡C base pairs is sufficient to support intercalative binding, but a run of four A=T base pairs suffices to define a groove-binding site. For groove binding, time-resolved Raman methods have led to a model which assumes that Cu(T4) binds face on in the major groove. In strictest terms, the model pertains to a covalently bound form of the excited state namely the exciplex with the nanosecond lifetime. However, CD studies involving hairpin hosts suggest that the four-coordinate ground state has a similar footprint. At the same time, nucleolytic studies involving other, more redox-active metal complexes of H<sub>2</sub>T4 have led to a model which assumes that the groove-bound form binds edge on within the minor groove. The two models have evolved from different kinds of experiments, and both modes of groove binding may occur. Either adduct is likely to involve partial melting of the DNA in the vicinity of the ligand; thus, the resulting groove structure may differ from that of canonical B-form DNA. The other side of the coin is that local rigidity should disfavor groove binding and encourage intercalative binding, consistent with the requirement of G≡C base pairs.

## VI. Acknowledgments

The National Science Foundation supported this work through grant number CHE-9401238. The

names of co-workers appear in the reference list, but Denise Crites deserves special mention for critically reading the text.

## VII. References

- Schleif, R. F.; Wensink, P. C. *Practical Methods in Molecular Biology*; Springer-Verlag: New York, 1981; pp 90–92.
- Nielsen, P. E.; Møllegaard, N. E.; Jeppesen, C. *Nucleic Acids Res.* **1990**, *18*, 3847–3851.
- Breiner, K. M.; Daugherty, M. A.; Oas, T. G.; Thorp, H. H. *J. Am. Chem. Soc.* **1995**, *117*, 11673–11679.
- Henderson, B. W.; Dougherty, T. J. *Photochem. Photobiol.* **1992**, *55*, 145–157.
- Barton, J. K. *Science* **1986**, *233*, 727–734.
- Calladine, C. R.; Drew, H. R. *Understanding DNA*; Academic Press: London, 1992.
- Turro, N. J.; Barton, J. K.; Tomalia, D. A. *Acc. Chem. Res.* **1991**, *24*, 332–340.
- Franklin, C. A.; Fry, J. V.; Collins, J. G. *Inorg. Chem.* **1996**, *35*, 7541–7545.
- Fry, J. V.; Collins, J. G. *Inorg. Chem.* **1997**, *36*, 2919–2921.
- Wilson, W. D. In *Nucleic Acids in Chemistry and Biology*; Blackburn, G. M.; Gait, M. J., Eds.; Oxford University Press: Oxford, 1990; pp 295–236.
- Wang, A. H. J.; Nathans, J.; van der Marel, G.; van Boom, J. H.; Rich, A. *Nature (London)* **1978**, *276*, 471–474.
- Lipscomb, L. A.; Zhou, F. X.; Presnell, S. R.; Woo, R. J.; Peek, M. E.; Plaskon, R. R.; Williams, L. D. *Biochemistry* **1996**, *35*, 2818–2823.
- Takahara, P. M.; Rosenzweig, A. C.; Frederick, C. A.; Lippard, S. J. *Nature* **1995**, *377*, 649–652.
- Huang, H.; Zhu, L.; Reid, B. R.; Drobny, G. P.; Hopkins, P. B. *Science* **1995**, *270*, 1842–1845.
- Pasternack, R. F.; Gurreri, S.; Lauceri, R.; Purrello, R. *Inorg. Chim. Acta* **1996**, *246*, 7–12.
- Tamilarasan, R.; McMillin, D. R. *Inorg. Chem.* **1990**, *29*, 2798–2802.
- Sigman, D. S.; Mazumder, A.; Perrin, D. M. *Chem. Rev.* **1993**, *93*, 2295–2316.
- Sigman, D. S.; Landgraf, R.; Perrin, D. M.; Pearson, L. *Met. Ions Biol. Syst.* **1996**, *33*, 485–513.
- Sigman, D. S.; Graham, D. R.; D'Aurora, V.; Stern, A. M. *J. Biol. Chem.* **1979**, *254*, 12269–12272.
- Kuwabara, M.; Yoon, C.; Goyné, T.; Thederahn, T.; Sigman, D. S. *Biochemistry* **1986**, *25*, 7401–7408.
- Thederahn, T. B.; Kuwabara, M. D.; Larsen, T. A.; Sigman, D. S. *J. Am. Chem. Soc.* **1989**, *111*, 4941–4946.
- Veal, J. M.; Rill, R. L. *Biochemistry* **1991**, *30*, 1132–1140.
- Sigman, D. S. *Acc. Chem. Res.* **1986**, *19*, 180–186.
- Tamilarasan, R.; McMillin, D. R.; Liu, F. In *Metal-DNA Chemistry*; Tullius, T. D., Ed.; ACS Symposium Series 402; American Chemical Society: Washington, DC, 1989; pp 48–58.
- Ceulemans, A.; Vanquickenborne, L. G. *J. Am. Chem. Soc.* **1981**, *103*, 2238–2241.
- Phifer, C. C.; McMillin, D. R. *Inorg. Chem.* **1986**, *25*, 1329–1333.
- Everly, R. M.; McMillin, D. R. *J. Phys. Chem.* **1991**, *95*, 9071–9075.
- Sakaki, S.; Mizutani, H.; Kase, Y. *Inorg. Chem.* **1992**, *31*, 4575–4581.
- Daul, C.; Schläpfer, C. W.; Goursot, A.; Pénigault, E.; Weber, J. *Chem. Phys. Lett.* **1981**, *78*, 304–310.
- Pallenberg, A. J.; Koenig, K. S.; Barnhart, D. M. *Inorg. Chem.* **1995**, *34*, 2833–2840.
- McGarvey, J. J.; Bell, S. E. J.; Gordon, K. C. *Inorg. Chem.* **1988**, *27*, 4003–4006.
- Eggleston, M. K.; McMillin, D. R.; Koenig, K. S.; Pallenberg, A. J. *Inorg. Chem.* **1997**, *36*, 172–176.
- Everly, R. M.; Ziesse, R.; Suffert, J.; McMillin, D. R. *Inorg. Chem.* **1991**, *30*, 559–561.
- Shinozaki, K.; Kaizu, Y. *Bull. Chem. Soc. Jpn.* **1994**, *67*, 2435–2439.
- Klemens, F. K.; Fanwick, P. E.; Bibler, J. K.; McMillin, D. R. *Inorg. Chem.* **1989**, *28*, 3076–3079.
- Eggleston, M. K.; Fanwick, P. E.; Pallenberg, A. J.; McMillin, D. R. *Inorg. Chem.* **1997**, *36*, 4007–4010.
- Palmer, C. E. A.; McMillin, D. R.; Kirmaier, C.; Holten, D. *Inorg. Chem.* **1987**, *26*, 3167–3170.
- Burke, P. J.; Henrick, K.; McMillin, D. R. *Inorg. Chem.* **1982**, *21*, 1881–1886.
- Elder, R. C.; Lunte, C. E.; Rahman, A. F. M. M.; Kirchhoff, J. R.; Dewald, H. D.; Heineman, W. R. *J. Electroanal. Chem.* **1988**, *240*, 361–364.
- McMillin, D. R.; Kirchhoff, J. R.; Goodwin, K. V. *Coord. Chem. Rev.* **1985**, *64*, 83–92.
- Stacy, E. M.; McMillin, D. R. *Inorg. Chem.* **1990**, *29*, 393–396.
- Horvath, A.; Stevenson, K. L. *Coord. Chem. Rev.* **1996**, *153*, 57–82.
- Dietrich-Buchecker, C. O.; Marnot, P. A.; Sauvage, J. P.; Kirchhoff, J. R.; McMillin, D. R. *J. Chem. Soc., Chem. Commun.* **1983**, 513–515.
- Everly, R. M.; McMillin, D. R. *Photochem. Photobiol.* **1989**, *50*, 711–716.
- Buckner, M. T.; McMillin, D. R. *J. Chem. Soc., Chem. Commun.* **1978**, 759–761.
- Mazumder, A.; Perrin, D. M.; McMillin, D. R.; Sigman, D. S. *Biochemistry* **1994**, *33*, 2262–2268.
- (a) Tamilarasan, R.; Ropartz, S.; McMillin, D. R. *Inorg. Chem.* **1988**, *27*, 4082–4084. (b) Mokul'skii, M. A.; Kaiparova, K. A.; Mokul'skaya, T. D. *Mol. Biol. (Moscow)* **1972**, *6*, 714–731.
- Pyle, A. M.; Rehmann, J. P.; Meshoyrer, R.; Kumar, C. V.; Turro, N. J.; Barton, J. K. *J. Am. Chem. Soc.* **1989**, *111*, 3051–3058.
- Graham, D. R.; Sigman, D. S. *Inorg. Chem.* **1984**, *23*, 4188–4191.
- Barton, J. K.; Basile, L. A.; Danishefsky, A.; Alexandrescu, A. *Proc. Natl. Acad. Sci., U.S.A.* **1984**, *81*, 1961–1965.
- Liu, F.; Meadows, K. A.; McMillin, D. R. *J. Am. Chem. Soc.* **1993**, *115*, 6699–6704.
- McMillin, D. R.; Hudson, B. P.; Liu, F.; Sou, J.; Berger, D. J.; Meadows, K. A. In *Photosensitive Metal-Organic Systems*; Kutal, C.; Serpone, N., Eds.; Adv. Chem. Series 238; American Chemical Society: Washington, DC, 1993; pp 211–231.
- Bradley, D. F.; Wolf, M. K. *Proc. Natl. Acad. Sci., U.S.A.* **1959**, *45*, 944–952.
- Meadows, K. A.; Liu, F.; Sou, J.; Hudson, B. P.; McMillin, D. R. *Inorg. Chem.* **1993**, *32*, 2919–2923.
- Gabbay, E. J.; Scofield, R. E.; Baxter, C. S. *J. Am. Chem. Soc.* **1973**, *95*, 7850–7857.
- Goldstein, B. M.; Barton, J. K.; Berman, H. M. *Inorg. Chem.* **1986**, *25*, 842–847.
- (a) Meadows, K. A.; Liu, F.; Hudson, B. P.; McMillin, D. R. *Inorg. Chem.* **1993**, *32*, 4663–4666. (b) McMillin, D. R.; Liu, F.; Meadows, K. A.; Aldridge, T. K.; Hudson, B. P. *Coord. Chem. Rev.* **1994**, *132*, 105–112.
- Norden, B.; Lincoln, P.; Åkerman, B.; Tuite, E. *Met. Ions Biol. Syst.* **1996**, *33*, 177–252.
- Ravikanth, M.; Chandrashekar, T. K. *Struct. Bonding (Berlin)* **1995**, *82*, 105–188.
- Ford, K. G.; Pearl, L. H.; Neidle, S. *Nucleic Acids Res.* **1987**, *15*, 6553–6562.
- Eaton, S. S.; Fishwild, D. M.; Eaton, G. R. *Inorg. Chem.* **1978**, *17*, 1542–1545.
- Kaufmann, T.; Shamsai, B.; Lu, R. S.; Bau, R.; Miskelly, G. M. *Inorg. Chem.* **1995**, *34*, 5073–5079.
- Collins, D. M.; Hoard, J. L. *J. Am. Chem. Soc.* **1970**, *92*, 3761–3771.
- Scheidt, W. R.; Lee, Y. J. *Struct. Bonding (Berlin)* **1987**, *64*, 1–70.
- Fiel, R. J.; Datta-Gupta, N.; Mark, E. H.; Howard, J. C. *Cancer Res.* **1981**, *41*, 3543–3545.
- Meng, G. G.; James, B. R.; Skov, K. A.; Korbelik, M. *Can. J. Chem.* **1994**, *72*, 2447–2457.
- Munson, B. R.; Fiel, R. J. *Nucleic Acids Res.* **1992**, *20*, 1315–1319.
- Pasternack, R. F.; Gibbs, E. J. *Met. Ions Biol. Syst.* **1996**, *33*, 367–397.
- Praseuth, D.; Gaudemer, A.; Verlhac, J. B.; Kraljić, I.; Sissoëff, I.; Guille, E. *Photochem. Photobiol.* **1986**, *44*, 717–724.
- Verlhac, J. B.; Gaudemer, A.; Kraljić, I. *Nouv. J. Chim.* **1984**, *8*, 401–406.
- Kelly, J. M.; Murphy, M. J.; McConnell, D. J.; OhUigin, C. *Nucleic Acids Res.* **1985**, *13*, 167–184.
- Brun, A. M.; Harriman, A. *J. Am. Chem. Soc.* **1994**, *116*, 10383–10393.
- Hyun, K. M.; Choi, S. D.; Lee, S.; Kim, S. K. *Biochim. Biophys. Acta* **1997**, *1334*, 312–316.
- Ake, R. L.; Gouterman, M. *Theor. Chim. Acta* **1969**, *15*, 20–42.
- Gouterman, M. In *The Porphyrins*; Dolphin, D., Ed.; Academic: New York, 1978; Vol. iii, part A, pp 1–165.
- Longuet-Higgins, H. C.; Rector, C. W.; Platt, J. R. *J. Chem. Phys.* **1950**, *18*, 1174–1181.
- Kobayashi, T.; Huppert, D.; Straub, K. D.; Rentzepis, P. M. *J. Chem. Phys.* **1979**, *70*, 1720–1726.
- Asano, M.; Kaizu, Y.; Kobayashi, H. *J. Chem. Phys.* **1988**, *89*, 6567–6576.
- Spellane, P. J.; Gouterman, M.; Antipas, A.; Kim, S.; Liu, Y. C. *Inorg. Chem.* **1980**, *19*, 386–391.
- Smith, B. E.; Gouterman, M. *Chem. Phys. Lett.* **1968**, *2*, 517–519.
- Antipas, A.; Dolphin, D.; Gouterman, M.; Johnson, E. C. *J. Am. Chem. Soc.* **1978**, *100*, 7705–7709.
- Henriksson, A.; Roos, B.; Sundbom, M. *Theor. Chim. Acta* **1972**, *27*, 303–313.
- Case, D. A.; Karplus, M. *J. Am. Chem. Soc.* **1977**, *99*, 6182–6194.
- Yan, X.; Holten, D. *J. Phys. Chem.* **1988**, *92*, 5982–5986.

- (85) Eastwood, D.; Gouterman, M. *J. Mol. Spectrosc.* **1969**, *30*, 437–458.
- (86) Asano-Someda, M.; Kaizu, Y. *J. Photochem. Photobiol. A (Chem.)* **1995**, *87*, 23–29.
- (87) Fleischer, E. B.; Miller, C. K.; Webb, L. E. *J. Am. Chem. Soc.* **1964**, *86*, 2342–2347.
- (88) Scheidt, W. R.; Kastner, M. E.; Hatano, K. *Inorg. Chem.* **1978**, *17*, 706–710.
- (89) Sapunov, V. V.; Tsvirko, M. P. *Opt. Spectrosc.* **1980**, *49*, 152–156.
- (90) Harriman, A. *J. Chem. Soc., Faraday Trans. 2* **1981**, *77*, 1281–1291.
- (91) Cunningham, K. L.; McNett, K. M.; Pierce, R. A.; Davis, K. A.; Harris, H. H.; Falk, D. M.; McMillin, D. R. *Inorg. Chem.* **1997**, *36*, 608–613.
- (92) Curtis, J. C.; Sullivan, B. P.; Meyer, T. J. *Inorg. Chem.* **1983**, *22*, 224–236.
- (93) Assour, J. M. *J. Chem. Phys.* **1965**, *43*, 2477–2489.
- (94) Portela, C. F.; Magde, D.; Traylor, T. G. *Inorg. Chem.* **1993**, *32*, 1313–1320.
- (95) Ohtaki, H.; Inada, Y.; Funahashi, S.; Tabata, M.; Ozutsumi, K.; Nakajima, K. *J. Chem. Soc., Chem. Commun.* **1994**, 1023–1025.
- (96) Kunkely, H.; Vogler, A. *Inorg. Chim. Acta* **1997**, *254*, 417–419.
- (97) Jeoung, S. C.; Kim, D.; Cho, D. W.; Yoon, M. *J. Phys. Chem.* **1995**, *99*, 5826–5833.
- (98) Jentzen, W.; Unger, E.; Song, X. Z.; Jia, S. L.; Turowska-Tyrk, I.; Schweitzer-Stenner, R.; Dreybrodt, W.; Scheidt, W. R.; Shelnutt, J. A. *J. Phys. Chem. A* **1997**, *101*, 5789–5798.
- (99) Kim, D.; Holten, D.; Gouterman, M. *J. Am. Chem. Soc.* **1984**, *106*, 2793–2798.
- (100) Hudson, B. P.; Sou, J.; Berger, D. J.; McMillin, D. R. *J. Am. Chem. Soc.* **1992**, *114*, 8997–9002.
- (101) Liu, F.; Cunningham, K. L.; Uphues, W.; Fink, G. W.; Schmolt, J.; McMillin, D. R. *Inorg. Chem.* **1995**, *34*, 2015–2018.
- (102) Gutmann, V. *Chimia* **1977**, *31*, 1–7.
- (103) Apanasevich, P. A.; Chirvony, V. S.; Kruglik, S. G.; Kvach, V. V.; Orlovich, V. A. In *Laser Applications in Life Sciences*; Akhmanov, S. A., Poroshina, M. Y., Eds.; Proceedings of SPIE, Vol. 1403, Part I SPIE.; SPIE: Bellingham, WA, 1991; pp 195–211.
- (104) Kruglik, S. G.; Apanasevich, P. A.; Chirvony, V. S.; Kvach, V. V.; Orlovich, V. A. *J. Phys. Chem.* **1995**, *99*, 2978–2995.
- (105) de Paula, J. C.; Walters, V. A.; Jackson, B. A.; Cardozo, K. J. *Phys. Chem.* **1995**, *99*, 4373–4379.
- (106) Jeoung, S. C.; Eom, H. S.; Kim, D.; Cho, D. W.; Yoon, M. *J. Phys. Chem. A* **1997**, *101*, 5412–5417.
- (107) Kruglik, S. G.; Ermolenkov, V. V.; Shvedko, A. G.; Orlovich, V. A.; Galievsky, V. A.; Chirvony, V. S.; Otto, C.; Turpin, P. Y. *Chem. Phys. Lett.* **1997**, *270*, 293–298.
- (108) Fiel, R. J. *J. Biomol. Struct. Dyn.* **1989**, *6*, 1259–1274.
- (109) Marzilli, L. G. *New J. Chem.* **1990**, *14*, 409–420.
- (110) Gibbs, E. J.; Tinoco, I., Jr.; Maestre, M. F.; Ellinas, P. A.; Pasternack, R. F. *Biochem. Biophys. Res. Commun.* **1988**, *157*, 350–358.
- (111) Pasternack, R. F.; Gibbs, E. J.; Villafranca, J. J. *Biochemistry* **1983**, *22*, 2406–2414.
- (112) Geacintov, N. E.; Ibanez, V.; Rougee, M.; Benasson, R. V. *Biochemistry* **1987**, *26*, 3087–3092.
- (113) Strickland, J. A.; Marzilli, L. G.; Wilson, W. D. *Biopolymers* **1990**, *29*, 1307–1323.
- (114) Strickland, J. A.; Banville, D. L.; Wilson, W. D.; Marzilli, L. G. *Inorg. Chem.* **1987**, *26*, 3398–3406.
- (115) Pasternack, R. F.; Gibbs, E. J.; Villafranca, J. J. *Biochemistry* **1983**, *22*, 5409–5417.
- (116) Sehlstedt, U.; Kim, S. K.; Carter, P.; Goodisman, J.; Vollano, J. F.; Nordén, B.; Dabrowiak, J. C. *Biochemistry* **1994**, *33*, 417–426.
- (117) Raner, G.; Goodisman, J.; Dabrowiak, J. C. In *Metal-DNA Chemistry*; Tullius, T., Ed; ACS Symposium Series 402; American Chemical Society: Washington, DC, 1989; pp 74–89.
- (118) Ward, B.; Skorobogaty, A.; Dabrowiak, J. C. *Biochemistry* **1986**, *25*, 7827–7833.
- (119) Ford, K.; Fox, K. R.; Neidle, S.; Waring, M. J. *Nucleic Acids Res.* **1987**, *15*, 2221–2234.
- (120) Marzilli, L. G.; Banville, D. L.; Zon, G.; Wilson, W. D. *J. Am. Chem. Soc.* **1986**, *108*, 4188–4192.
- (121) Gibbs, E. J.; Maurer, M. C.; Zhang, J. H.; Reiff, W. M.; Hill, D. T.; Malicka-Blaszkiewicz, M.; McKinnie, R. E.; Liu, H.-Q.; Pasternack, R. F. *J. Inorg. Biochem.* **1988**, *32*, 39–65.
- (122) Dougherty, G.; Pasternack, R. F. *Biophys. Chem.* **1992**, *44*, 11–19.
- (123) Fiel, R. J.; Munson, B. R. *Nucleic Acids Res.* **1980**, *8*, 2835–2842.
- (124) Hui, X.; Gresh, N.; Pullman, B. *Nucleic Acids Res.* **1990**, *18*, 1109–1114.
- (125) Greiner, S. P.; Kreilick, R. W.; Marzilli, L. G. *J. Biomol. Struct. Dyn.* **1992**, *9*, 837–851.
- (126) Pitié, M.; Pratviel, G.; Bernadou, J.; Meunier, B. *Proc. Natl. Acad. Sci. U.S.A.* **1992**, *89*, 3967–3971.
- (127) Carvlin, M. J.; Fiel, R. J. *Nucleic Acids Res.* **1983**, *11*, 6121–6139.
- (128) Eggleston, M. K.; Crites, D. K.; McMillin, D. R.; Submitted for publication.
- (129) (a) Schneider, J. H.; Odo, J.; Nakamoto, K. *Nucleic Acids Res.* **1988**, *16*, 10323–10338. (b) Turpin, P. Y.; Chinsky, L.; Laigle, A.; Tsuboi, M.; Kincaid, J. R.; Nakamoto, K. *Photochem. Photobiol.* **1990**, *51*, 519–525.
- (130) Chinsky, L.; Turpin, P. Y.; Al-Obaidi, A. H. R.; Bell, S. E. J.; Hester, R. E. *J. Phys. Chem.* **1991**, *95*, 5754–5756.
- (131) Strahan, G. D.; Lu, D.; Tsuboi, M.; Nakamoto, K. *J. Phys. Chem.* **1992**, *96*, 6450–6457.
- (132) Mojzes, P.; Chinsky, L.; Turpin, P. Y. *J. Phys. Chem.* **1993**, *97*, 4841–4847.
- (133) Kruglik, S. G.; Galievsky, V. A.; Chirvony, V. S.; Apanasevich, P. A.; Ermolenkov, V. V.; Orlovich, V. A.; Chinsky, L.; Turpin, P. Y. *J. Phys. Chem.* **1995**, *99*, 5732–5741.

CR9601167

